



6-2016

A General Code to Simulate the Effect of Indirect Lightning on Overhead Lines Using EMTP-Type Programs

Hasan Jameel Hasan
Western Michigan University

Follow this and additional works at: https://scholarworks.wmich.edu/masters_theses



Part of the Electrical and Computer Engineering Commons

Recommended Citation

Hasan, Hasan Jameel, "A General Code to Simulate the Effect of Indirect Lightning on Overhead Lines Using EMTP-Type Programs" (2016). *Masters Theses*. 733.

https://scholarworks.wmich.edu/masters_theses/733

This Masters Thesis-Open Access is brought to you for free and open access by the Graduate College at ScholarWorks at WMU. It has been accepted for inclusion in Masters Theses by an authorized administrator of ScholarWorks at WMU. For more information, please contact wmu-scholarworks@wmich.edu.



A GENERAL CODE TO SIMULATE THE EFFECT OF INDIRECT LIGHTNING ON
OVERHEAD LINES USING EMTP-TYPE PROGRAMS

by

Hasan Jameel Hasan

A thesis submitted to the Graduate College
in partial fulfillment of the requirements
for the degree of Master of Science in Electrical Engineering
Electrical and Computer Engineering
Western Michigan University
June 2016

Thesis Committee:

Pablo Gomez, Ph.D., Chair

Ikhlas Abdel-Qader, Ph.D.

Massood Atashbar, Ph.D.

A GENERAL CODE TO SIMULATE THE EFFECT OF INDIRECT LIGHTNING ON OVERHEAD LINES USING EMTP-TYPE PROGRAMS

Hasan Jameel Hasan, M.S.E.

Western Michigan University, 2016

In this thesis, a general code is obtained to allow the simulation of the transient response of transmission lines excited by a nearby lightning stroke using EMTP-type programs, namely PSCAD and ATP.

Initially, the frequency domain modeling of single phase and multiconductor transmission lines is described and assessed by means of several application examples. As a second stage, the transmission line model is used to implement an illuminated transmission line model (line excited by an electromagnetic field excitation) using Taylor's formulation. Then, a general code is developed in MATLAB to obtain the response of a field excited line; this effect is included by means of terminal current sources connected at the ends of the line. Finally, these terminal current sources are used in EMTP – type programs to reproduce the transient response of a transmission line excited by indirect lightning. Several application examples are included to demonstrate the accuracy and versatility of the code.

© 2016 Hasan Jameel Hasan

ACKNOWLEDGMENTS

I would like to express my appreciation to several people who have helped and supported my graduate studies and this thesis work. Firstly, I would like to thank my thesis supervisor and committee chair, Dr. Pablo Gomez, for his valuable advice, support, and feedback throughout my project. Secondly, I would like to thank Dr. Ikhlas Abdel-Qader, and Dr. Massood Atashbar, for their participation on the thesis committee, and for their evaluation and feedback. Next, I would like to thank my devoted wife and sons for their love and patience, my parents for their prayers, and my father-in-law, Haje Hamid, for his financial support. Finally, I would like to thank all of the friends I have met in the U.S. and at WMU for their camaraderie during this chapter of my life.

Hasan Jameel Hasan

TABLE OF CONTENTS

ACKNOWLEDGMENTS	ii
LIST OF TABLES	vii
LIST OF FIGURES	viii
CHAPTER 1	1
INTRODUCTION	1
1.1 Introduction	1
1.2 Objectives.....	2
1.3 Literature Review	2
1.4 Thesis Structure.....	5
CHAPTER 2	7
OVERVIEW ON TRANSMISSION LINE MODELING	7
2.1 Introduction.....	7
2.2 Solving Telegrapher Equations in the Frequency Domain.....	8
2.2.1 Characteristic Admittance and Impedance	9
2.2.2 Transfer Matrix Model (ABCD Matrix) for Single Phase Transmission Line	10
2.2.3 Admittance Matrix Model for Single Phase Transmission Line (Y_{bus}).....	11

Table of Contents - Continued

2.2.4	Transfer Matrix Model (ABCD Matrix) for Multiconductor Transmission Line.....	12
2.2.5	Admittance Matrix Model for Multiconductor Transmission Line (\mathbf{Y}_{bus}) ..	13
2.3	Applications	13
2.3.1	Single Phase Transmission Line	14
2.3.2	Multiconductor Transmission Line.....	15
2.4	Conclusions.....	18
CHAPTER 3		19
MODELING OF AN ILLUMINATED TRANSMISSION LINE		19
3.1	Introduction.....	19
3.2	Illuminated Transmission Line Model.....	19
3.2.1	Incident Field	19
3.2.2	Distributed Sources	20
3.2.3	Lumped Sources.....	22
3.2.4	Two-Port Model for an Illuminated Transmission Line	24
3.3	Applications	25
3.3.1	Single Phase Line Excited by Distributed Series Voltage Sources	25

Table of Contents - Continued

3.3.2	Single Phase Line Excited by Distributed Series Voltage and Shunt Current Sources	27
3.3.3	Multiconductor Line Excited by Distributed Series Voltage Sources	29
3.4	Conclusions.....	32
CHAPTER 4		33
COMPUTATION OF INCIDENT ELECTROMAGNETIC FIELD AND DESCRIPTION OF GENERAL CODE WITH TEST CASES		33
4.1	Introduction.....	33
4.2	Computation of Incident Electromagnetic Field.....	34
4.3	Description of General Code	36
4.4	Test Case in ATP Program and Validation with NLT	45
4.4.1	Application Example for Single Phase Line in ATP	45
4.4.2	Application Example for Multiconductor Line in ATP.....	48
4.5	Test Case in PSCAD Program and Validation with NLT.....	51
4.5.1	Application Example for Single Phase Line in PSCAD.....	51
4.5.2	Application Example for Multiconductor Line in PSCAD.....	54
4.6	Conclusions.....	56

Table of Contents - Continued

CHAPTER 5	57
CONCLUSIONS AND FUTURE WORK	57
BIBLIOGRAPHY	59
Appendix A: Electrical Parameters of the Transmission Line.....	63
Appendix B: Numerical Laplace Transform.....	68

LIST OF TABLES

2.1 Parameters for the single phase transmission line example.....	14
2.2 Parameters for multiconductor transmission line example.....	16
3.1 Parameters for single phase line excited by distributed series voltage sources	26
3.2 Parameters for multiconductor line excited by distributed series voltage sources	29
4.1 Parameters for single phase line	46
4.2 Lightning channel data.....	46
4.3 Parameters for multiconductor line.....	49
4.4 Lightning channel data.....	49

LIST OF FIGURES

2.1 Equivalent circuit of the transmission line per unit length	8
2.2 Boundary conditions for single phase transmission line.....	10
2.3 Boundary conditions for three phase transmission line	11
2.4 Admittance matrix mode.....	12
2.5 Single phase line configuration with unit step excitation	15
2.6 Transient analysis for the single phase transmission line example.....	15
2.7 Multiconductor line configuration with unit step excitation.....	16
2.8 Transient analysis for multiconductor transmission line example – Phase A	17
2.9 Transient analysis for multiconductor transmission line example – Phase B.....	17
2.10 Transient analysis for multiconductor transmission line example – Phase C.....	18
3.1 Field excited multiconductor line configuration.....	20
3.2 Representation of an illuminated line segment.....	23
3.3 Illuminated line representation through equivalent sources	23
3.4 Model of the illuminated line by injected current sources at the line terminals	25
3.5 Circuit developed in ATP for an illuminated line excited by distributed series voltage sources.....	26
3.6 Induced voltage at the ends of a single phase line	27

List of Figures – Continued

3.7 Circuit developed in ATP for an illuminated line excited by distributed series voltage and shunt current sources	28
3.8 Induced voltage at the ends of the single phase line	28
3.9 Circuit developed in ATP for a multiconductor illuminated line excited by distributed series voltage sources.....	30
3.10 Induced voltage at the ends of phase A for multiconductor line	31
3.11 Induced voltage at the ends of phase B for multiconductor line.....	31
3.12 Induced voltage at the ends of phase C for multiconductor line.....	32
4.1 Geometrical configuration for the electromagnetic coupling between the lightning channel and a transmission line	36
4.2 Block diagram for the general code	37
4.3 Coordinates of the point of impact.....	38
4.4 Circuit developed in ATP for an illuminated single phase line	40
4.5 Circuit developed in ATP for an illuminated multiconductor line	40
4.6 Steps a and b for the inclusion of external currents from text file in ATP	41
4.7 Step c for the inclusion of external currents from text file in ATP.....	41
4.8 Circuit developed in PSCAD for an illuminated single phase line.....	42
4.9 Circuit developed in PSCAD for an illuminated multiconductor line.....	42

List of Figures – Continued

4.10 Step a for the inclusion of external currents from text file in PSCAD	43
4.11 Steps b and c for the inclusion of external currents from text file in PSCAD	44
4.12 Step d for the inclusion of external currents from text file in PSCAD	44
4.13 Induced voltages at the ends of a single phase line for point of impact P(150,50) – ATP	47
4.14 Induced voltages at the ends of a single phase line for point of impact P(300,60) – ATP	47
4.15 Induced voltages at the ends of a single phase line for point of impact P(400,70) – ATP	48
4.16 Induced voltages at the ends of a multiconductor line for point of impact P(25,50) – ATP	50
4.17 Induced voltages at the ends of a multiconductor line for point of impact P(50,60) – ATP	50
4.18 Induced voltages at the ends of a multiconductor line for point of impact P(175,70) – ATP	51
4.19 Induced voltages at the ends of a single phase line for point of impact P(150,50) – PSCAD	52
4.20 Induced voltages at the ends of a single phase line for point of impact P(300,60) – PSCAD	53

List of Figures – Continued

4.21 Induced voltages at the ends of a single phase line for point of impact P(400,70) – PSCAD.....	53
4.22 Induced voltages at the ends of a multiconductor line for point of impact P(25,50) – PSCAD.....	54
4.23 Induced voltages at the ends of a multiconductor line for point of impact P(50,60) – PSCAD.....	55
4.24 Induced voltages at the ends of a multiconductor line for point of impact P(175,70) – PSCAD.....	55
A.1 Method of images.....	64
A.1 Penetration depth representation	66

CHAPTER 1

INTRODUCTION

1.1 Introduction

An electromagnetic transient occurs when there is a sudden change of electromagnetic energy in a power system. This change can be caused by lightning or switching [1]. The effect of lightning induces overvoltages in transmission lines and can be classified in direct and indirect lightning phenomena. Direct strokes usually affect the towers and conductors of transmission lines. In a well-designed transmission system, the ground conductors are generally the ones hit by direct lightning strokes, although a small percentage of strokes can still hit the phase conductors. On the other hand, indirect lightning corresponds to lightning strokes to ground in the proximity of the transmission line. As expected, direct lightning strokes produce higher transient overvoltages than indirect lightning. However, the effect of incident electromagnetic fields from indirect lightning strokes is important for the design of protection and insulation elements. In addition, indirect lightning is a much more frequent phenomenon than direct lightning. The incident electromagnetic field representing the nearby lightning stroke depends on variables related to the location of the line (point of impact) and the return stroke current, according to the formulation developed by Master and Uman [2]- [4].

1.2 Objectives

- Implementing a frequency domain model of an illuminated (field-excited) transmission line, for both single phase and multiconductor cases.
- Applying the illuminated line model to obtain terminal currents related to an incident field from an indirect lightning stroke.
- Creating a general code to produce the excitations required by transient simulation programs ATP and PSCAD to reproduce the transient response of a transmission line excited by indirect lightning (single phase and multiconductor cases).

1.3 Literature Review

The following are some important works related to the modeling of a transmission line excited by an indirect electromagnetic field, also known as illuminated line.

In 1965, D. C. Taylor modeled and analyzed the effect of a nonuniform electromagnetic field on a two-wire transmission line [5].

In 1976, C. Paul [6] described a transmission line model excited by an external electromagnetic source. From the previous study, the response of a two-wire transmission line illuminated by a nonuniform electromagnetic field was extended to multiconductor lines.

In 1980, Agrawal et al. derived the time-domain equations of multiconductor transmission lines excited by a nonuniform electromagnetic field [7]. Two formulations were discussed depending on the definition of the line voltage. The first formulation is

scattered-voltage, in which the sources are introduced in only one equation. The second one is total-voltage formulation, in which the sources representing the incident electric fields contain time derivatives and spatial integrals.

In 1993, Rachidi [8] reviewed and discussed different formulations for field-to-line electromagnetic coupling. A new formulation was derived to evaluate such coupling when the excitation source is defined experimentally (the source terms are expressed in terms of magnetic excitation field).

In 1994, V. Cooray [9] compared the Rusck model [10] and the wave antenna model [7] to estimate the lightning induced overvoltages on transmission lines. He concluded that the Rusck model can only be successful when an electromagnetic field is generated in a specific location such that the contribution of the vector potential to the horizontal field is zero.

In 1994 and 1995, C. Paul described and implemented an illuminated line model in the simulation program SPICE. The incident fields were represented by series voltage and shunt current sources connected at the receiving end of the line [11], [12].

In 1995, C. A. Nucci et al. [13] compared and discussed the field-to-line coupling model defined by Chowdhuri and Gross with the model by Agrawal, Price and Gurbaxani. It is shown that the model from Chowdhuri-Gross is incomplete because the source term due to the contribution of the magnetic induction is omitted. On the other hand, the Agrawal model completely describes the coupling between the lightning

electromagnetic field and the line. This model is expressed in terms of total voltage and is equivalent to the model by Taylor.

In 1997, M. Omid et al. [14] studied the time and frequency domain responses of a transmission line excited by incident electromagnetic fields for uniform and nonuniform cases. For uniform lines, the inverse of the chain matrix is used to define the corresponding model. For nonuniform lines, the modeling approach followed consists of dividing the line in uniform segments and computing the cascaded connection of chain matrices. The external field is represented by lumped current sources connected at the line terminals.

In 1998, V. Cooray and V. Scuka [15] investigated the validity of different approximations applied in the computation of lightning induced overvoltages on transmission lines.

In 2001, I. Erdin et al. [16] implemented a model for incident field coupling to multiconductor transmission lines in the time domain. The model is based on the rational approximation of the exponential matrix describing the telegrapher's equations and semi-analytical rational approximation of convolution functions. This model can be easily used in SPICE like simulators for transient analysis, and it is in the form of ordinary differential equations.

In 2005, P. Gomez et al. [17] presented two methods in the frequency domain for analyzing nonuniform transmission lines excited by incident electromagnetic fields. In the first method, the cascade connection of chain matrices of uniform line segments is

applied. The second method is based on the derivation of the chain matrix (a space-variant linear system). The numerical Laplace transform (NLT) was used to obtain the solution in time domain.

In 2005 and 2006, G. Shinh et al. presented an algorithm for transient analysis to obtain the effect of electromagnetic fields on multiconductor lines with frequency dependent parameters [18], [19]. The model was developed in the simulation program SPICE. The incident electromagnetic fields were represented by voltage and current sources at the ends of the line.

In 2009, P. Gomez and J. C. Escamilla [26] presented a method in the frequency domain for analyzing nonuniform multiconductor transmission lines excited by indirect lightning by means of terminal current sources connected at the ends of the line.

In 2013, P. Gomez and J. C. Escamilla [3] included surge arresters in simulation of field excited transmission lines using the frequency domain model described in [26].

In 2015, R. Nuricumbo-Guillén et al. [24] computed the transient voltage and current profiles along multiconductor transmission lines excited by indirect lighting using a two-dimensional definition of the numerical Laplace transform (NLT).

1.4 Thesis Structure

Chapter 1, Introduction: This chapter includes introduction, objectives, literature review, and thesis structure.

Chapter 2, Overview on Transmission Line Modeling: The transfer matrix model (ABCD matrix) and admittance matrix model are described and implemented in this

chapter. In addition, some application examples are shown to validate the models implemented.

Chapter 3, Modeling of an Illuminated Transmission Line: The effect of an incident field on a transmission line is discussed in this chapter. Distributed and lumped sources are used to implement an illuminated transmission line model. The model from this chapter is applied in different examples to obtain the effect of distributed sources along transmission lines, comparing the results with the transient simulation program ATP.

Chapter 4, Computation of Incident Electromagnetic Field and Description of General Code: This chapter discusses the computation of incident electromagnetic fields from a nearby lightning stroke on a transmission line. This chapter also describes the implementation and steps required for the application of a general code to produce the excitations required by ATP and PSCAD to simulate the transient response of a field excited transmission line.

Chapter 5, Conclusions and Future Work: The main results and contributions of this thesis are summarized.

CHAPTER 2

OVERVIEW ON TRANSMISSION LINE MODELING

2.1 Introduction

The power transmission line is one of the major components of electrical power systems. Transmission lines transport the electrical energy from power plants to the consumers with minimum losses.

The correct evaluation of transmission systems in transient and steady states require the use of modern modeling and simulation tools, which involve an accurate and efficient computation of electrical parameters (per-unit-length parameters).

The equivalent circuit of a transmission line for transient analysis is shown in Figure 2.1. It contains a series resistance (R) due to the resistivity of the conductor, a series inductance (L) due to the magnetic flux produced by the current flow along the conductor, a shunt capacitance (C) due to the electric field between the conductor and the reference plane, and a shunt conductance (G) due to dielectric losses. All of these parameters are given per unit length of the line. For overhead lines, the shunt conductance is usually omitted because it has a very small effect compared with the series resistance (the air is considered a very good dielectric) [20], [17], [21].

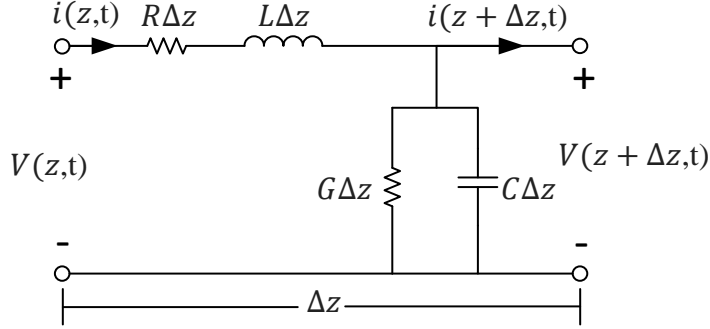


Figure 2.1 Equivalent circuit of the transmission line per unit length

2.2 Solving Telegrapher Equations in the Frequency Domain

The Telegrapher equations define the propagation of traveling waves along a transmission line. These equations are given in the frequency domain by:

$$-\frac{dV(z,s)}{dz} = ZI(z,s) \quad (2.1)$$

$$-\frac{dI(z,s)}{dz} = YV(z,s) \quad (2.2)$$

where $V(z,s)$ and $I(z,s)$ are the voltages and currents in the Laplace domain at point z of the line, while Z and Y represent the series impedance and shunt admittance per unit length, respectively. The computation of these parameters is described in Appendix A. By combining (2.1) and (2.2) a second order uncoupled matrix arrangement is obtained as [22]:

$$\frac{d^2}{dz^2} \begin{bmatrix} V(z,s) \\ I(z,s) \end{bmatrix} = \begin{bmatrix} ZY & 0 \\ 0 & YZ \end{bmatrix} \begin{bmatrix} V(z,s) \\ I(z,s) \end{bmatrix} \quad (2.3)$$

The general solution of (2.3) for voltage and current is given by:

$$V(z, s) = C_1 e^{-\gamma z} + C_2 e^{\gamma z} \quad (2.4)$$

$$I(z, s) = C_3 e^{-\gamma z} + C_4 e^{\gamma z} \quad (2.5)$$

where C_1 , C_2 , C_3 and C_4 are integration constants and γ is the propagation constant defined as:

$$\gamma = \sqrt{ZY} = \sqrt{(R + sL)(G + sC)} \quad (2.6)$$

2.2.1 Characteristic Admittance and Impedance

To solve equations (2.4) and (2.5) the concept of characteristic admittance is used.

Substituting equation (2.4) in (2.1) and solving for current I :

$$I(z, s) = -Z^{-1} \frac{d(C_1 e^{-\gamma z} + C_2 e^{\gamma z})}{dz} = Y_o (C_1 e^{-\gamma z} + C_2 e^{\gamma z}) \quad (2.7)$$

Y_o is the characteristic admittance of the line. It defines the relationship between voltage and current waves. According to (2.7), Y_o is obtained from

$$Y_o = Z^{-1} \gamma \quad (2.8)$$

Substituting (2.6) in (2.8):

$$Y_o = \sqrt{\frac{Y}{Z}} \quad (2.9)$$

The characteristic impedance Z_o can be found from the inverse of the characteristic admittance Y_o as follows [22]:

$$Z_o = \frac{1}{Y_o} = \sqrt{\frac{Z}{Y}} \quad (2.10)$$

2.2.2 Transfer Matrix Model (ABCD Matrix) for Single Phase Transmission Line

Applying boundary conditions at the sending and receiving node of the line ($z = 0$ and $z = l$), as shown in Figure 2.2, the transfer matrix model of the line is obtained as follows [23] [22]:

$$\begin{bmatrix} V_l \\ I_l \end{bmatrix} = \begin{bmatrix} A & B \\ C & D \end{bmatrix} \begin{bmatrix} V_0 \\ I_0 \end{bmatrix} \quad (2.11)$$

where

$$A = \cosh(\gamma l) \quad (2.12)$$

$$B = -Z_o \sinh(\gamma l) \quad (2.13)$$

$$C = Y_o \sinh(\gamma l) \quad (2.14)$$

$$D = -\cosh(\gamma l) \quad (2.15)$$

V_0 and I_0 are the voltage and current at the sending node, V_l and I_l are the voltage and current at the receiving node, and l is the length of the transmission line.

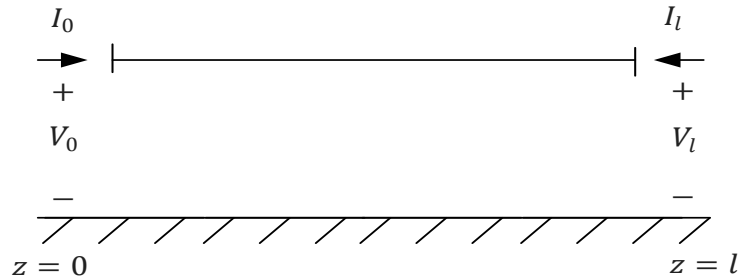


Figure 2.2 Boundary conditions for single phase transmission line

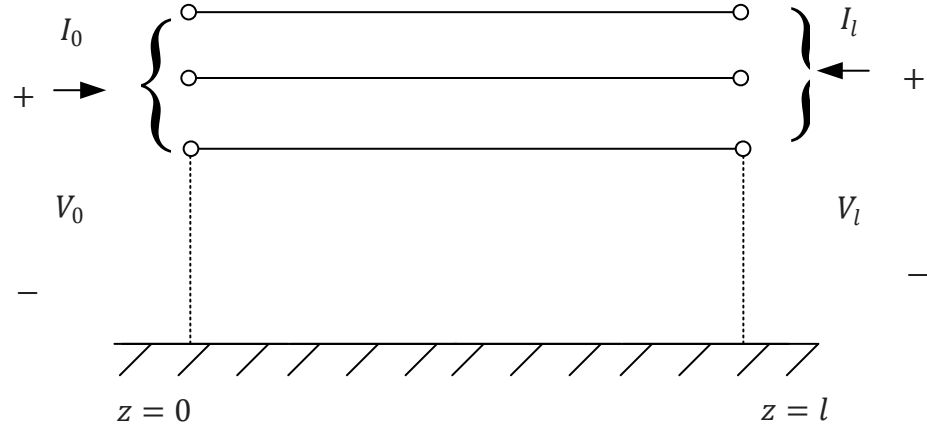


Figure 2.3 Boundary conditions for three phase transmission line

2.2.3 Admittance Matrix Model for Single Phase Transmission Line (Y_{bus})

After some algebraic manipulations of the transfer matrix model defined by (2.11), an admittance matrix model is obtained as follows:

$$\begin{bmatrix} I_o \\ I_l \end{bmatrix} = \begin{bmatrix} Y_{SS} & -Y_{SR} \\ -Y_{RS} & Y_{RR} \end{bmatrix} \begin{bmatrix} V_0 \\ V_l \end{bmatrix} \quad (2.16)$$

where

$$Y_{SS} = Y_{RR} = Y_0 \coth(\gamma l) \quad (2.17)$$

$$Y_{SR} = Y_{RS} = Y_0 \operatorname{csch}(\gamma l) \quad (2.18)$$

Y_{SS} , Y_{SR} , Y_{RS} , and Y_{RR} are the elements of the admittance matrix model [22]. The two-port representation of this model is shown in Figure 2.4.

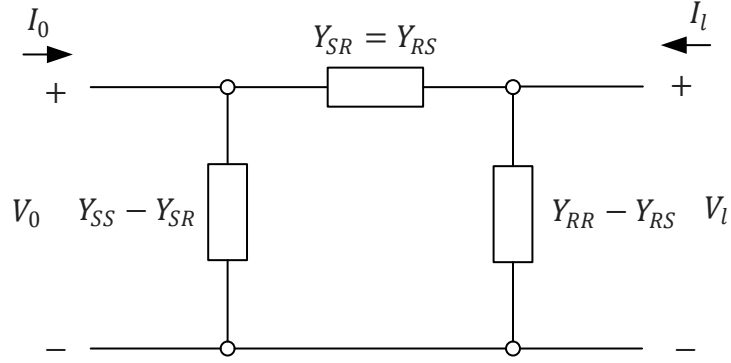


Figure 2.4 Admittance matrix model

2.2.4 Transfer Matrix Model (ABCD Matrix) for Multiconductor Transmission Line

For the multiconductor case, parameters \mathbf{Z} and \mathbf{Y} from the telegrapher equations are matrices of size $n \times n$, where n is number of conductors. Also, \mathbf{V} and \mathbf{I} are column vectors of length n . Applying modal decomposition to decouple the system, the transfer matrix model of a multiconductor line is defined, as follows:

$$\begin{bmatrix} \mathbf{V}_l \\ \mathbf{I}_l \end{bmatrix} = \begin{bmatrix} \mathbf{A} & \mathbf{B} \\ \mathbf{C} & \mathbf{D} \end{bmatrix} \begin{bmatrix} \mathbf{V}_0 \\ \mathbf{I}_0 \end{bmatrix} \quad (2.19)$$

where

$$\mathbf{A} = \cosh(\boldsymbol{\Psi}l) \quad (2.20)$$

$$\mathbf{B} = -\sinh(\boldsymbol{\Psi}l)\mathbf{Z}_0 \quad (2.21)$$

$$\mathbf{C} = \mathbf{Y}_0 \sinh(\boldsymbol{\Psi}l) \quad (2.22)$$

$$\mathbf{D} = -\mathbf{Y}_0 \cosh(\boldsymbol{\Psi}l)\mathbf{Z}_0 \quad (2.23)$$

Ψ is the constant propagation matrix of the line, defined as follows:

$$\Psi = \mathbf{M}\sqrt{\lambda}\mathbf{M}^{-1} \quad (2.24)$$

λ and \mathbf{M} are the eigenvalue and eigenvector matrices of the product \mathbf{ZY} , respectively. \mathbf{Z}_0 is the characteristic impedance matrix of the line, and \mathbf{Y}_0 is the characteristic admittance matrix of the line defined as follows [3]:

$$\mathbf{Y}_0 = \mathbf{Z}^{-1}\Psi \quad (2.25)$$

2.2.5 Admittance Matrix Model for Multiconductor Transmission Line (\mathbf{Y}_{bus})

By means of an algebraic manipulation of (2.192.192.19), the admittance matrix model of a multiconductor transmission line is obtained [3]:

$$\begin{bmatrix} \mathbf{I}_o \\ \mathbf{I}_l \end{bmatrix} = \begin{bmatrix} \mathbf{Y}_{SS} & -\mathbf{Y}_{SR} \\ -\mathbf{Y}_{RS} & \mathbf{Y}_{RR} \end{bmatrix} \begin{bmatrix} \mathbf{V}_0 \\ \mathbf{V}_l \end{bmatrix} \quad (2.26)$$

where

$$\mathbf{Y}_{SS} = \mathbf{Y}_{RR} = \mathbf{Y}_0 \coth(\Psi l) \quad (2.27)$$

$$\mathbf{Y}_{SR} = \mathbf{Y}_{RS} = \mathbf{Y}_0 \operatorname{csch}(\Psi l) \quad (2.28)$$

The time domain response of the line is obtained by solving (2.26) for the voltages vector and transforming the solutions to the time domain by means of the inverse numerical Laplace transform, as described in Appendix B.

2.3 Applications

The transmission line modeling approach described in the previous sections is applied to two different cases. In the first one, a single phase transmission line is

analyzed. In the second application example, a multiconductor transmission line is considered. Both application examples were validated by means of electromagnetic transients program ATP.

2.3.1 Single phase transmission line

The first application example corresponds to a single phase line with the parameters listed in Table 2.1. These parameters do not represent any particular real transmission line; they are considered only for simulation purposes and validation of the model. A unit step voltage source is applied at the sending node of the line, while the receiving end is left open, as shown in Figure 2.5. Figure 2.6 shows the voltage at the receiving node obtained by the frequency domain model and compared with ATP.

Table 2.1 Parameters for the single phase transmission line example

Line length	100 km
Line height	30 m
Conductor radius	0.01 m
Ground resistivity	100 $\Omega\cdot\text{m}$
Conductor resistivity	$2.61\times 10^{-8} \Omega\cdot\text{m}$
Source voltage	1 p.u.
Observation Time	0.01 sec

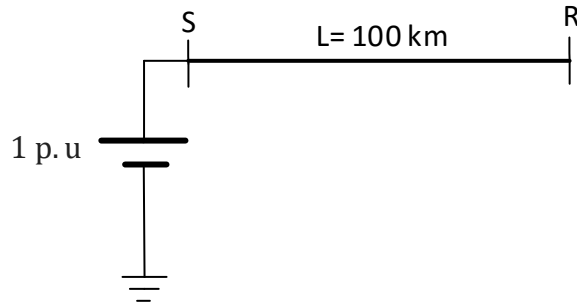


Figure 2.5 Single phase line configuration with unit step excitation

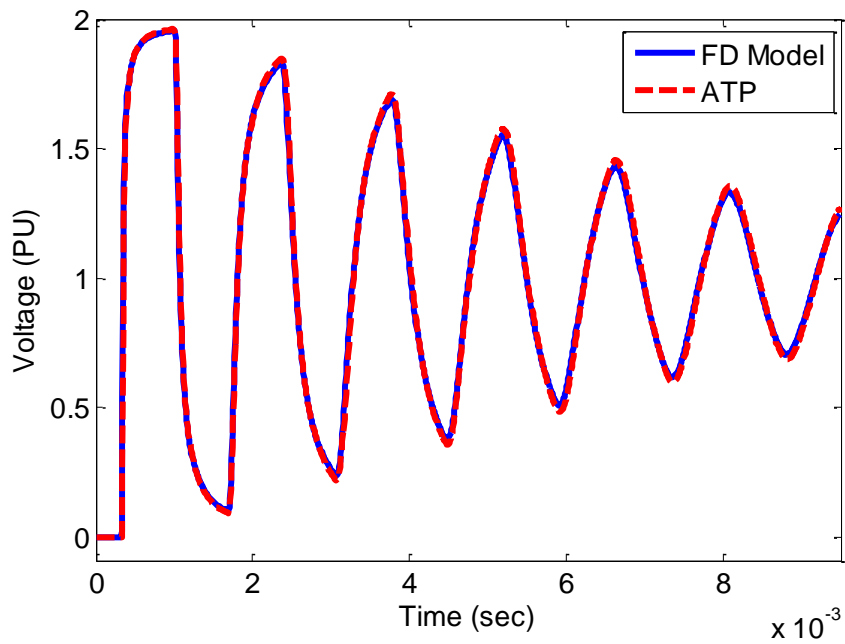


Figure 2.6 Transient voltage for the single phase transmission line example

2.3.2 Multiconductor Transmission Line

Table 2.2 shows the parameters for the simulation of a multiconductor line. As in the previous example, the parameters for this example are for validation purposes only and do not correspond to a real case. In this example, a unit step voltage source is

connected at phase A of the sending node, while the other two phases (B and C) are left open. Also, the receiving node is left open (all phases), as shown in Figure 2.7. Voltages at the receiving node obtained with the frequency domain model and validated with ATP for phases A, B, and C are shown in Figures 2.8, 2.9, and 2.10, respectively.

Table 2.2 Parameters for Multiconductor transmission line example

Line length	100 km
Line height	10 m
Distance between phases	1 m
Conductor radius	0.01 m
Ground resistivity	100 $\Omega\cdot\text{m}$
Conductor resistivity	2.61×10^{-8} $\Omega\cdot\text{m}$
Source voltage	1 p.u
Observation Time	0.01 sec

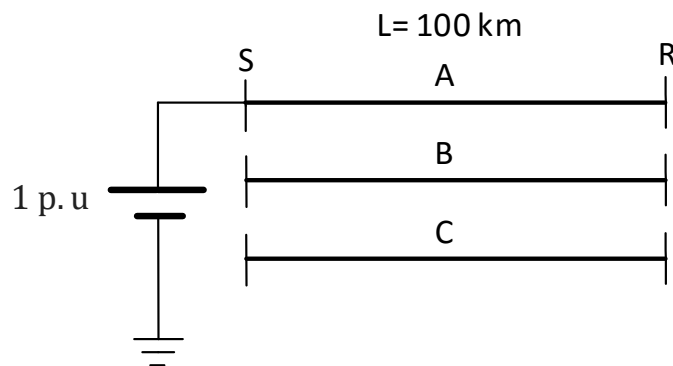


Figure 2.7 Multiconductors line configuration with unit step excitation

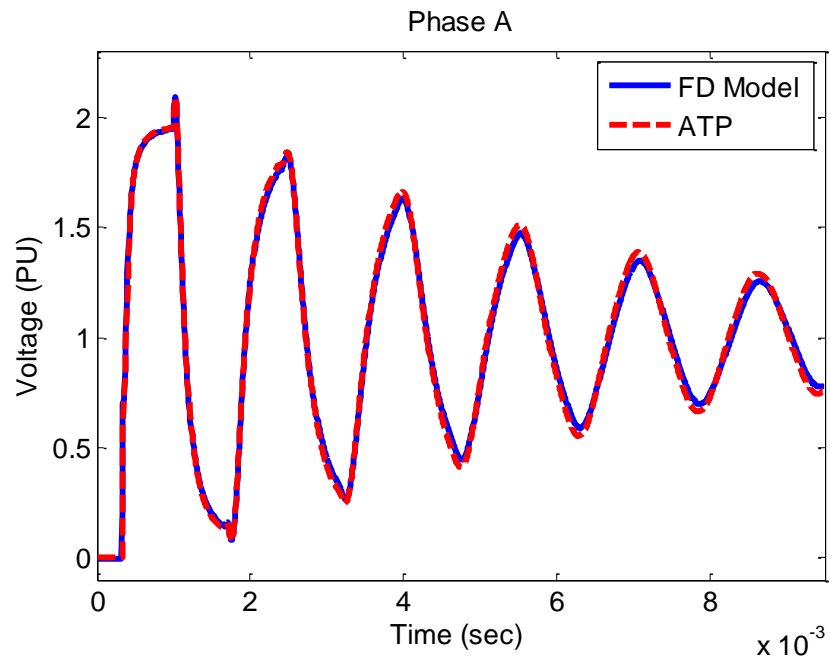


Figure 2.8 Transient voltage for multiconductor transmission line example - Phase A

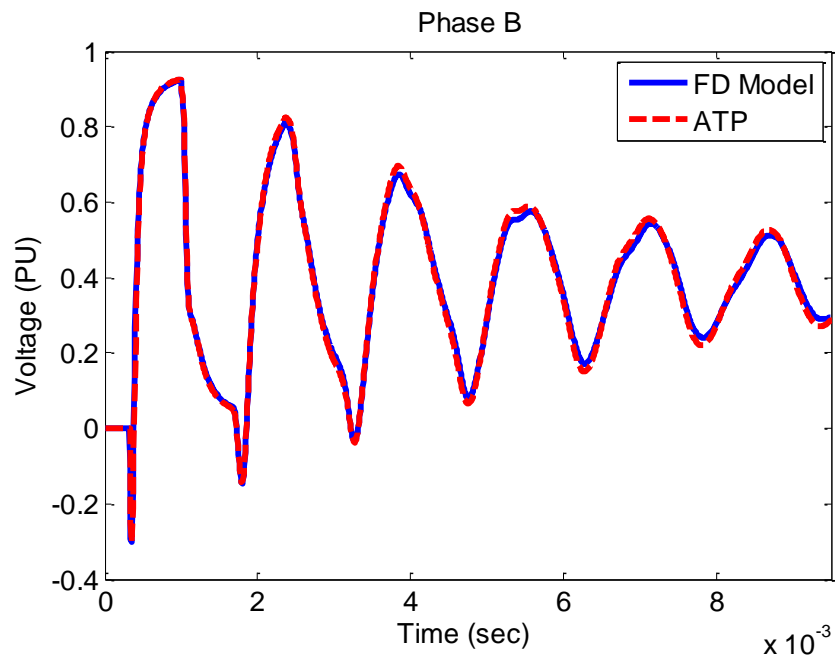


Figure 2.9 Transient voltage for multiconductor transmission line example - Phase B

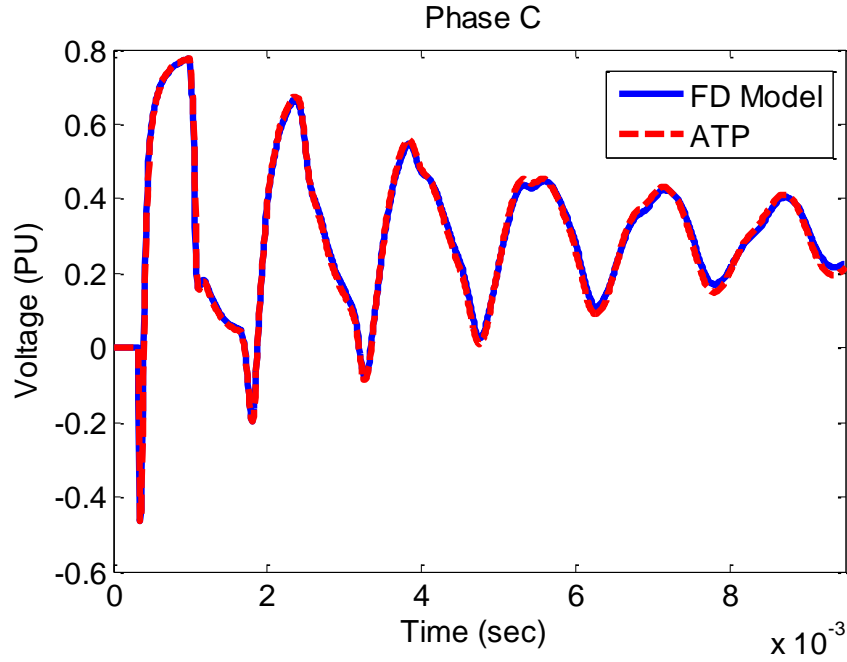


Figure 2.10 Transient voltage for multiconductor transmission line example - Phase C

2.4 Conclusions

This chapter described the frequency domain modeling of single phase and multiconductor transmission lines for electromagnetic transient analysis. According to the application examples, the results from the FD model are very similar to the simulation software ATP. In addition, Figures 2.6 and 2.8 demonstrate that the transient voltage at the receiving node of an open ended line reaches approximately two times the applied voltage. On the other hand, Figures 2.9 and 2.10 show the transient coupling voltage phases when only one phase is excited. The model described in this chapter will be used in Chapters 3 and 4 to simulate the electromagnetic coupling between a transmission line and an indirect lightning stroke.

CHAPTER 3

MODELING OF AN ILLUMINATED TRANSMISSION LINE

3.1 Introduction

In a general sense, a transmission line excited by an external electromagnetic field from any source is known as an illuminated line. The most common formulations to model an illuminated line were defined by Taylor [5], Agrawal [7] and Rachidi [8]. These formulations provide equivalent results in terms of induced total voltages and currents, even though they take into account the electromagnetic coupling fields in different ways [3], [24]. The illuminated transmission line model described in this chapter is used in Chapter 4 to obtain the effect of indirect lightning on transmission lines.

3.2 Illuminated Transmission Line Model

The illuminated transmission line model implemented in this thesis is based on Taylor's formulation [5], which describes a transmission line excited by an external electromagnetic field by means of series voltage and shunt current sources distributed along the line [25], [26].

3.2.1 Incident Field

A transmission line excited by an incident electromagnetic field is considered, as shown in Figure 3.1. The external field can be included to the line model by means of voltage and current sources distributed along the line. As described in the following

sections, this modeling approach can be further simplified by means of an equivalent representation in which the effect of the incident field is included by means of current sources connected only at the line terminals [17], [4], [27]. Finally, the solution in the time domain is obtained by applying the inverse Numerical Laplace Transform (NLT) (see Appendix B).

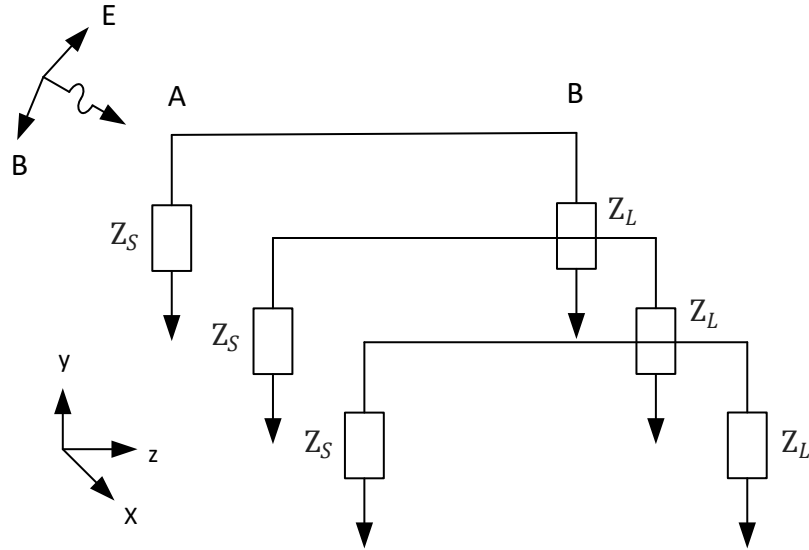


Figure 3.1 Field excited multiconductor line configuration

3.2.2 Distributed Sources

The Telegrapher Equations in the frequency domain for a multiconductor transmission line excited by an incident electromagnetic field are defined as follows [12], [21], [11], [26] [28]:

$$\frac{d\mathbf{V}(z, s)}{dz} = -\mathbf{Z}(z, s)\mathbf{I}(z, s) + \mathbf{V}_F(z, s) \quad (3.1)$$

$$\frac{d\mathbf{I}(z, s)}{dz} = -\mathbf{Y}(z)\mathbf{V}(z, s) + \mathbf{I}_F(z, s) \quad (3.2)$$

where s is the Laplace variable, $\mathbf{V}(z, s)$ and $\mathbf{I}(z, s)$ are the vectors of voltages and currents along the propagation axis z , $\mathbf{Z}(z, s)$ and $\mathbf{Y}(z, s)$ are the matrices of series impedance and shunt conductance per unit length. \mathbf{V}_F and \mathbf{I}_F are the vectors of distributed voltage and current sources from the incident electromagnetic field defined as follows [14], [8]:

$$\mathbf{V}_F(z, s) = s \begin{bmatrix} \vdots \\ \int_0^{h_i(z)} B_{x,i}(z, s) dy + E_{z,i}(0, s) \\ \vdots \end{bmatrix} \quad (3.3)$$

$$\mathbf{I}_F(z, s) = -\mathbf{Y}(z) \begin{bmatrix} \vdots \\ \int_0^{h_i(z)} E_{y,i}(z, s) dy \\ \vdots \end{bmatrix} \quad (3.4)$$

where $h_i(z)$ is the height of the i^{th} conductor; $B_{x,i}(z, s)$ and $E_{y,i}(z, s)$ are the transversal magnetic field and vertical electric field components on the i^{th} conductor in the Laplace domain, respectively. On the other hand, $E_{z,i}(0, s)$ is the horizontal electric field at ground level due to the finite ground conductivity [29], [8], [13], [30].

According to the matrix exponential concept and modal decomposition, the solution to (3.3) and (3.4) for a line segment Δz in terms of the chain matrix $\mathbf{\Phi}(\Delta z, s)$ is given by

$$\begin{bmatrix} \mathbf{V}(z + \Delta z, s) \\ \mathbf{I}(z + \Delta z, s) \end{bmatrix} = \mathbf{\Phi}(\Delta z, s) \begin{bmatrix} \mathbf{V}(z, s) \\ \mathbf{I}(z, s) \end{bmatrix} + \int_z^{z+\Delta z} \mathbf{\Phi}(z - \tau, s) \begin{bmatrix} \mathbf{V}_F(\tau, s) \\ \mathbf{I}_F(\tau, s) \end{bmatrix} d\tau \quad (3.5)$$

where

$$\Phi(\Delta z, s) = \begin{bmatrix} \cosh(\Psi \Delta z) & -\mathbf{Y}_0^{-1} \sinh(\Psi \Delta z) \\ -\mathbf{Y}_0 \sinh(\Psi \Delta z) & \cosh(\Psi \Delta z) \end{bmatrix} \quad (3.6)$$

Ψ is the phase domain constant propagation matrix of the line segment given by (2.24), and \mathbf{Y}_0 is the characteristic admittance matrix of the line segment.

Eq. (3.5) relates currents and voltages from one end of the line segment with the same variables on the other end. If the line segment is electrically small, the integral in (3.5) can be approximated as:

$$\int_z^{z+\Delta z} \Phi(z - \tau, s) \begin{bmatrix} \mathbf{V}_F(\tau, s) \\ \mathbf{I}_F(\tau, s) \end{bmatrix} d\tau \approx \begin{bmatrix} \mathbf{V}_F(z, s) \Delta z \\ \mathbf{I}_F(z, s) \Delta z \end{bmatrix} \quad (3.7)$$

According to (3.5) and (3.7), the effect of an electromagnetic field can be included in the line model by means of the addition of voltage and current sources at each line segment, as shown in Figure 3.2:

$$\begin{bmatrix} \mathbf{V}(z, s) \\ \mathbf{I}(z, s) \end{bmatrix} = \Phi(\Delta z, s) \begin{bmatrix} \mathbf{V}(z - \Delta z, s) \\ \mathbf{I}(z - \Delta z, s) \end{bmatrix} + \begin{bmatrix} \mathbf{V}_F(z, s) \Delta z \\ \mathbf{I}_F(z, s) \Delta z \end{bmatrix} \quad (3.8)$$

3.2.3 Lumped Sources

Applying boundary conditions at $z = 0$ and $z = l$, where l is the total length of the line, an equivalent illuminated line model can be obtained, in which the incident field is included by means of lumped sources connected only at the far end terminal of the line [17], [26], [3], [4]:

$$\begin{bmatrix} \mathbf{V}(l, s) \\ \mathbf{I}(l, s) \end{bmatrix} = \prod_{i=1}^M \mathbf{\Phi}^{(M+1-i)} \begin{bmatrix} \mathbf{V}(0, s) \\ \mathbf{I}(0, s) \end{bmatrix} + \begin{bmatrix} \mathbf{V}_{FT}(l, s) \\ \mathbf{I}_{FT}(l, s) \end{bmatrix} \quad (3.9)$$

where $\mathbf{\Phi}^i$ is the chain matrix for the i^{th} line segment. The first right hand side term of (3.9) corresponds to the total chain matrix for the unexcited line. The second term on the right hand side of (3.9) is defined as follows [3]:

$$\begin{bmatrix} \mathbf{V}_{FT}(l, s) \\ \mathbf{I}_{FT}(l, s) \end{bmatrix} = \sum_{i=1}^{M-1} \left\{ \prod_{n=0}^{M-i-1} \mathbf{\Phi}^{(M-n)} \begin{bmatrix} \mathbf{V}_F(i\Delta z, s)\Delta z \\ \mathbf{I}_F(i\Delta z, s)\Delta z \end{bmatrix} \right\} \quad (3.10)$$

When $\Delta z \rightarrow 0$, Eq. (3.10) becomes

$$\begin{bmatrix} \mathbf{V}_{FT}(l, s) \\ \mathbf{I}_{FT}(l, s) \end{bmatrix} = \int_0^l \mathbf{\Phi}(l-z, s) \begin{bmatrix} \mathbf{V}_F(z, s) \\ \mathbf{I}_F(z, s) \end{bmatrix} dz \quad (3.11)$$

Eq. (3.10) corresponds to the convolution in z between the chain matrix of the line and the vector of distributed sources.

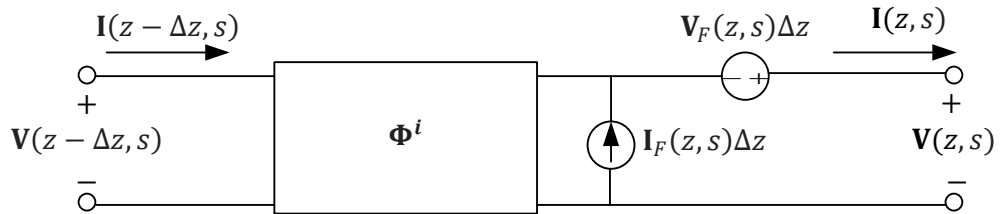


Figure 3.2 Representation of an illuminated line segment

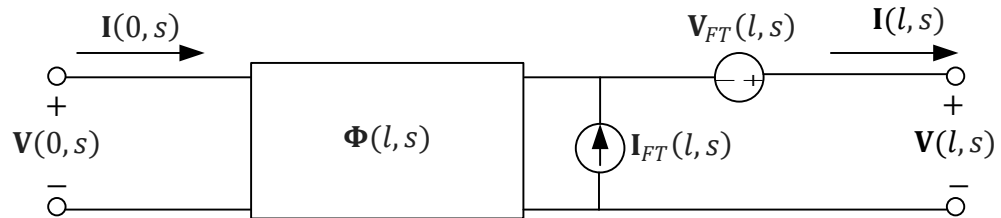


Figure 3.3 Illuminated line representation through equivalent sources

3.2.4 Two-Port Model for an Illuminated Transmission Line

After some algebraic manipulations of (3.9) and including admittances at the ends of the line, the following equation is obtained, which describes a two-port admittance matrix model with electromagnetic field excitation [24]:

$$\begin{bmatrix} \mathbf{I}(0, s) \\ \mathbf{I}(l, s) \end{bmatrix} = \begin{bmatrix} \mathbf{Y}_{SS} + \mathbf{Y}_S & -\mathbf{Y}_{SR} \\ -\mathbf{Y}_{RS} & \mathbf{Y}_{RR} + \mathbf{Y}_L \end{bmatrix} \begin{bmatrix} \mathbf{V}(0, s) \\ \mathbf{V}(l, s) \end{bmatrix} + \begin{bmatrix} \mathbf{I}_{SC}(0, s) \\ \mathbf{I}_{SC}(l, s) \end{bmatrix} \quad (3.12)$$

The direction of $\mathbf{I}(l, s)$ has been reversed considering injected currents for nodal analysis. The current sources connected at the ends of the line represent the incident electromagnetic field [3], as shown in Figure 3.4. The nodal admittance matrix elements are given by:

$$\begin{aligned} \mathbf{Y}_{SS} &= -\mathbf{\Phi}_{12}^{-1}\mathbf{\Phi}_{11} \\ \mathbf{Y}_{SR} = \mathbf{Y}_{RS} &= -\mathbf{\Phi}_{12}^{-1} = -\mathbf{\Phi}_{22}\mathbf{\Phi}_{12}^{-1}\mathbf{\Phi}_{11} + \mathbf{\Phi}_{21} \\ \mathbf{Y}_{RR} &= -\mathbf{\Phi}_{22}\mathbf{\Phi}_{12}^{-1} \end{aligned} \quad (3.13)$$

The current sources at the ends of the line are defined as follows:

$$\begin{aligned} \mathbf{I}_{SC}(0, s) &= -\mathbf{\Phi}_{12}^{-1}\mathbf{V}_{FT}(l, s) \\ \mathbf{I}_{SC}(l, s) &= \mathbf{\Phi}_{22}\mathbf{\Phi}_{12}^{-1}\mathbf{V}_{FT}(l, s) - \mathbf{I}_{FT}(l, s) \end{aligned} \quad (3.14)$$

where $\mathbf{\Phi}_{11}$, $\mathbf{\Phi}_{12}$, $\mathbf{\Phi}_{21}$, and $\mathbf{\Phi}_{22}$ are the elements of the chain matrix for the complete line.



Figure 3.4 Model of the illuminated line by injected current sources at line terminals

3.3 Applications

Three application examples are considered. In the first application example, a single phase line is excited by distributed series voltage sources. Then, the same line is excited by distributed series voltage and shunt current sources. Finally, a multiconductor line was excited by distributed series voltage sources. These examples are used to obtain the effect of distributed sources over the transmission lines. The distributed sources are unit steps and do not represent real cases.

3.3.1 Single Phase Line Excited by Distributed Series Voltage Sources

In this application example, a single phase line with the parameters listed in Table 3.1 is excited by distributed voltage sources. The line is divided in 20 equal segments, and the distributed series voltage sources are connected between those segments. The results obtained with the frequency domain model (denoted as NLT) are validated by means of electromagnetic transients program ATP. Figure 3.5 shows the line representation using software ATP. For (3.10), $V_F = 1$ p.u. and $I_F = 0$. Figure 3.6 shows

the induced voltage at the ends of the line (ends A and B). The results from both methods are very similar.

Table 3.1 Parameters for single phase line excited by distributed series voltage sources

Line length	600 m
Line height	30 m
Conductor radius	0.01 m
Ground resistivity	100 $\Omega\cdot\text{m}$
Number of line segments	20
Conductor resistivity	$2.61 \times 10^{-8} \Omega\cdot\text{m}$
Observation Time	0.03 ms
Resistances connected at both ends	522 Ω

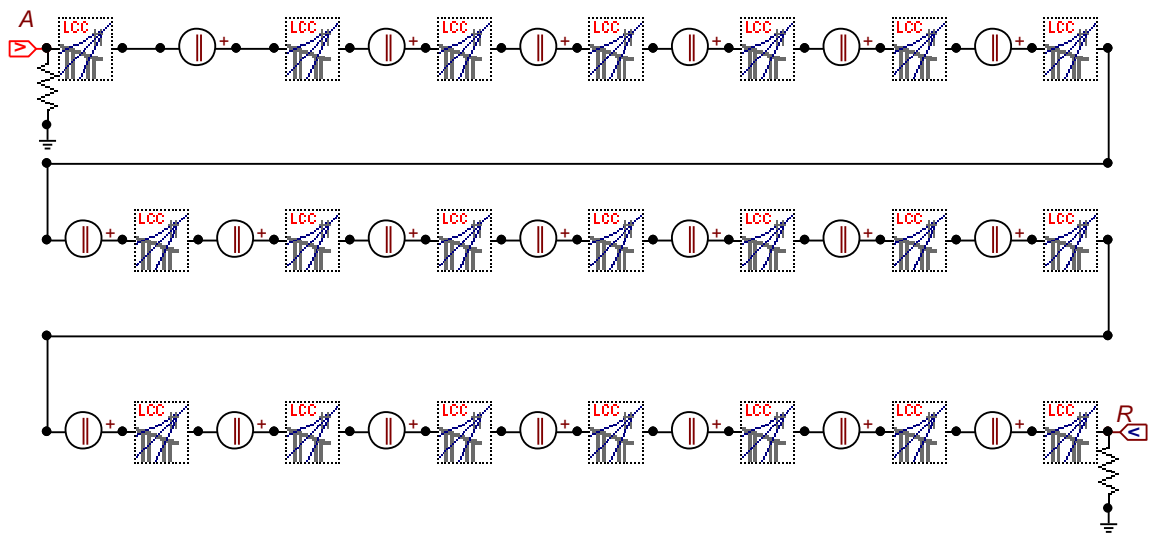


Figure 3.5 Circuit developed in ATP for an illuminated line excited by distributed series voltage sources

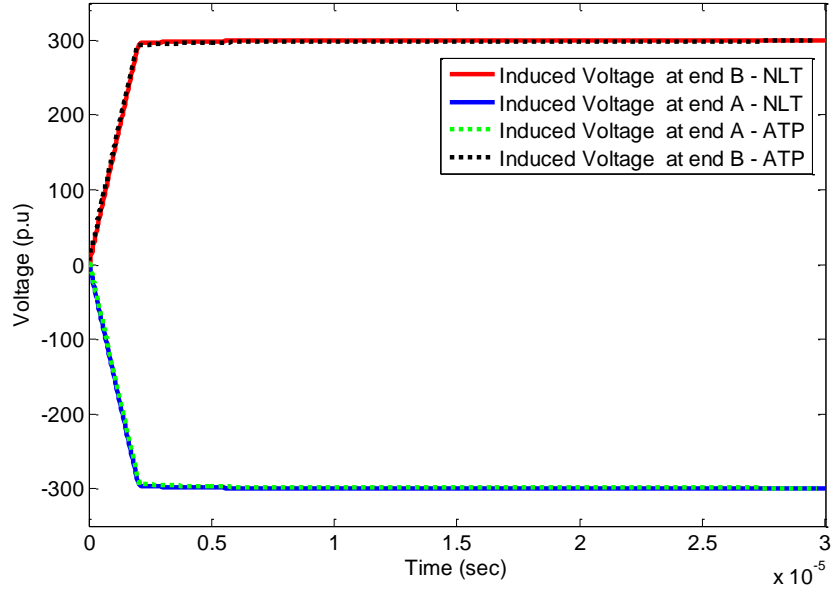


Figure 3.6 Induced voltage at the ends of a single phase line

3.3.2 Single Phase Line Excited by Distributed Series Voltage and Shunt Current

Sources.

The same line from the previous section is now excited by distributed voltage and current sources: $V_F = 1$ p.u and $I_F = 1$ p.u. Figure 3.7 shows the circuit developed in ATP. Figure 3.8 shows the induced voltage at the ends of A and B. Again, the results from the frequency domain model and from ATP are very similar.

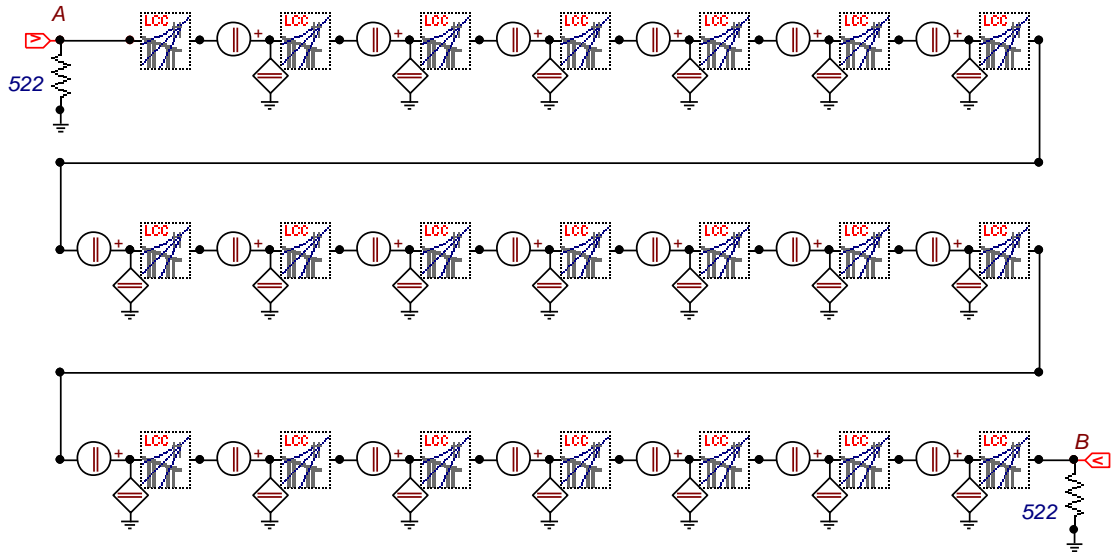


Figure 3.7 Circuit developed in ATP for an illuminated line excited by distributed series voltage and shunt current sources

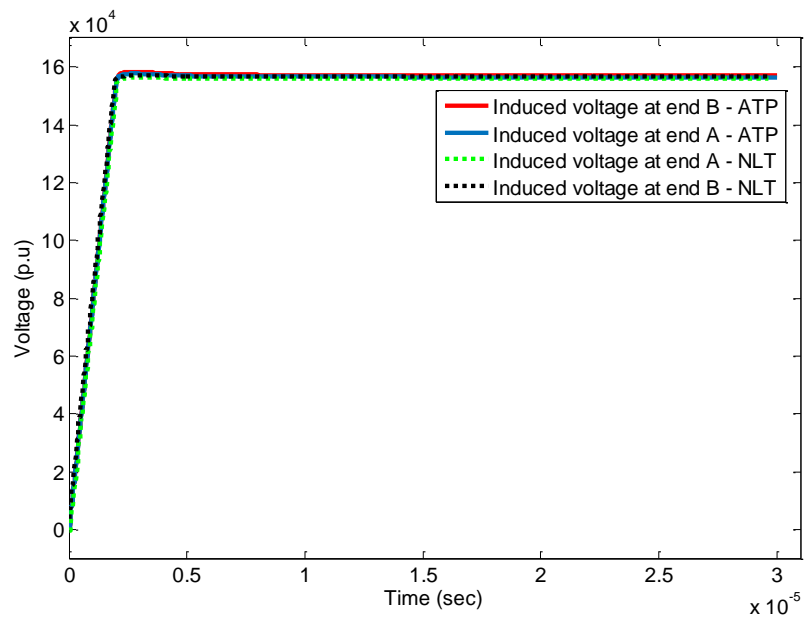


Figure 3.8 Induced voltage at the ends of the single phase line

3.3.3 Multiconductor Line Excited by Distributed Series Voltage Sources

As a third application example, a multiconductor line with the parameters listed in Table 3.2 is considered. The distributed sources per phase are $\mathbf{I}_F = 0$ and $\mathbf{V}_F = 1$ p. u. Eq. (3.12) was used to obtain the overvoltages for all phases of the line terminals. Figures 3.10, 3.11 and 3.12 illustrate the results from the frequency domain model and are validated with ATP by dividing the line in 20 equal segments, as shown in Figure 3.9.

Table 3.2 Parameters for multiconductor line excited by distributed series voltage sources

Line length	600 m
Line height	10 m
Conductor radius	0.01 m
Distance between phases	2 m
Number of line segments	20
Ground resistivity	100 $\Omega\cdot\text{m}$
Conductor resistivity	2.61×10^{-8} $\Omega\cdot\text{m}$
Observation Time	0.03 ms
Resistances connected at both ends	522 Ω

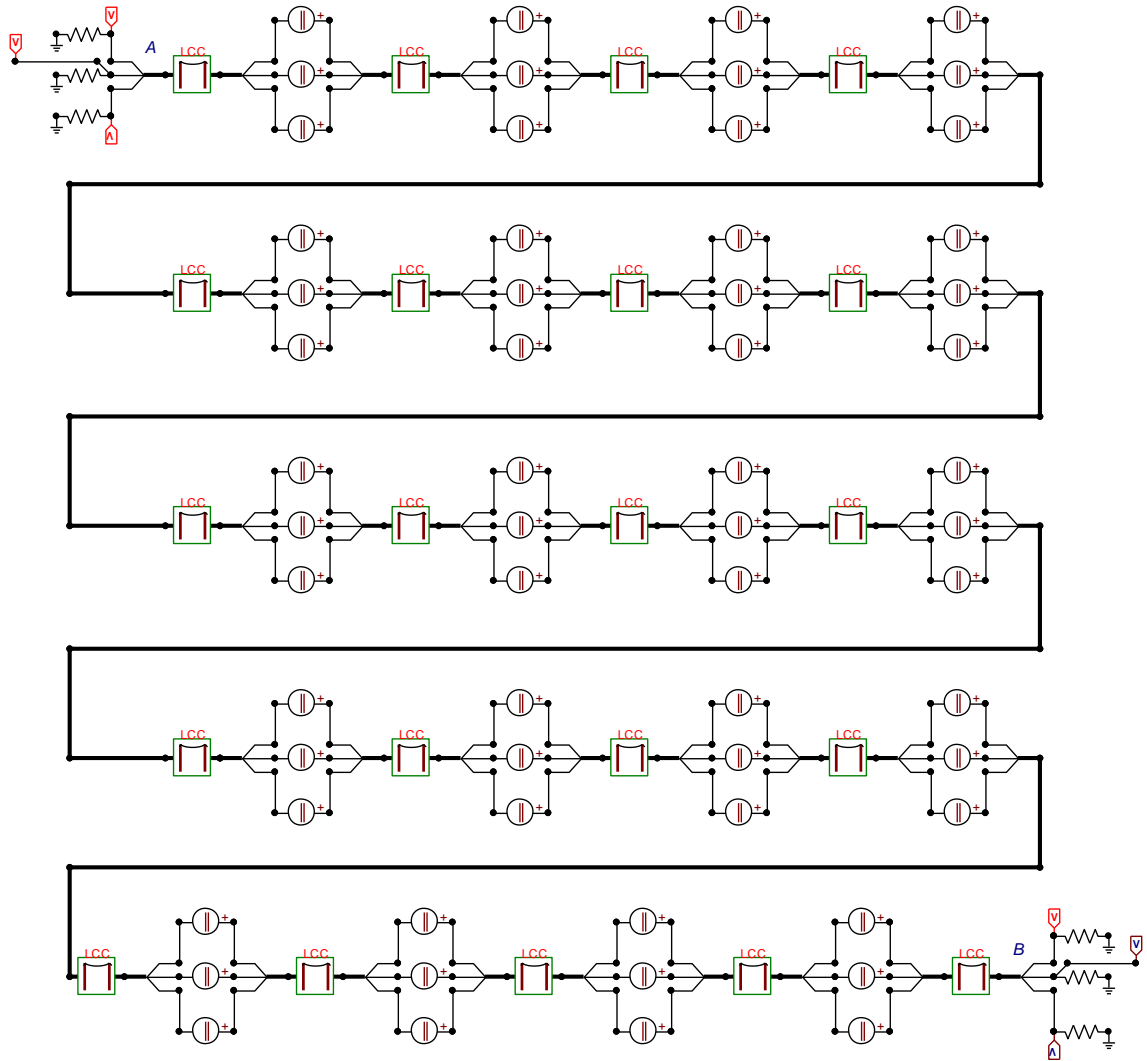


Figure 3.9 Circuit developed in ATP for a multiconductor illuminated line excited by distributed series voltage sources

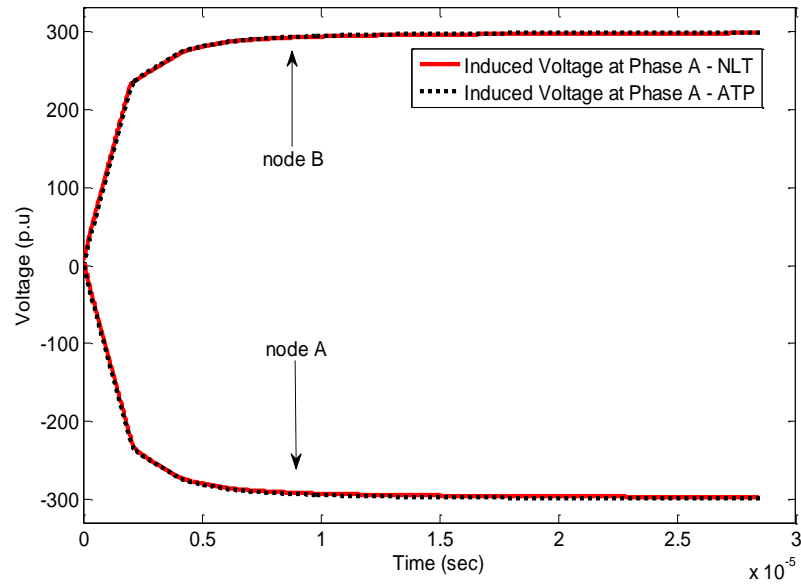


Figure 3.10 Induced voltage at the ends of phase A for multiconductor line

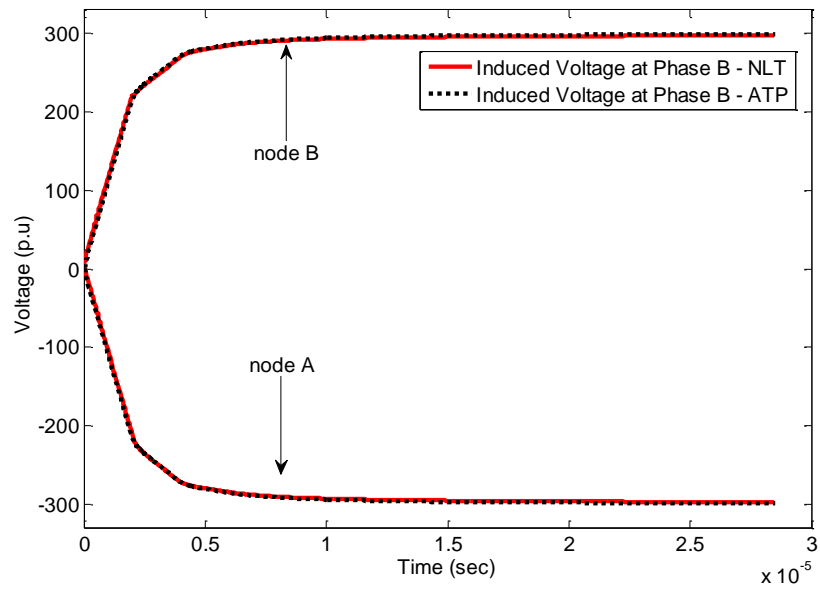


Figure 3.11 Induced voltage at the ends of phase B for multiconductor line

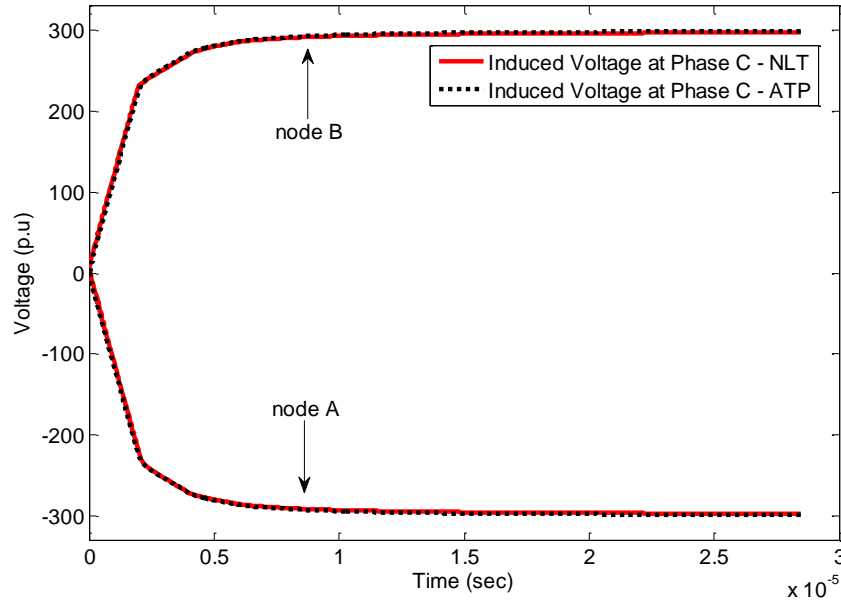


Figure 3.12 Induced voltage at the ends of phase C for multiconductor line

3.4 Conclusions

In this chapter, a frequency domain method for electromagnetic transient analysis of illuminated transmission lines has been described and implemented. To compute the effect of incident electromagnetic fields along the transmission line, distributed sources are included in the line model, which are further reduced to equivalent lumped sources by means of cascaded connection of chain matrices. By means of several test cases, a high level of agreement between the results from the frequency domain model and the simulation software ATP were observed.

CHAPTER 4

COMPUTATION OF INCIDENT ELECTROMAGNETIC FIELD AND DESCRIPTION OF GENERAL CODE WITH TEST CASES

4.1 Introduction

The effect of lightning on transmission and distribution lines can be classified in direct and indirect lightning phenomena. As expected, direct lightning strokes produce higher overvoltages than indirect strokes. However, since indirect lightning is much more frequent than direct lightning [31], [32], [19], [20], understanding the mechanism of the incident electromagnetic fields generated by indirect lightning strokes is necessary as part of the design and coordination of insulation and protection elements [9], [26], [24], [33]. The travelling waves produced by these electromagnetic fields along the transmission lines can affect the lines or any equipment connected to them.

This chapter describes the procedure followed to create a general code using MATLAB program to obtain terminal current sources representing indirect lightning, which are used as external sources for the EMTP-type programs ATP and PSCAD. This general code makes the computation of the effect of indirect lightning easier for the user, since a deep knowledge of the modeling approach behind this computation is not required. The inputs required by the user are the simulation data (observation time and number of samples), the transmission line data (geometrical and electrical parameters),

and the lightning data (stroke location, cloud's height, etc.). After introducing these data, the outputs received by the user are the terminal current vectors related to indirect lightning. Finally, the user can use these vectors in ATP or PSCAD to simulate the transient response of a transmission line excited by indirect lightning.

4.2 Computation of Incident Electromagnetic Field

The geometrical configuration in Figure 4.1 shows a transmission line excited by an incident electromagnetic field from a nearby lightning stroke. Assuming ground as a perfect conductor, Master and Uman defined the components of electric and magnetic field produced by a differential segment of a lightning channel [2]. The corresponding terms in the frequency domain are defined as follows [34], [3]:

$$dE_r(r, y, s) = \frac{dy}{4\pi\epsilon_0} I(y, s) \times \exp\left(-\frac{Rs}{s}\right) \left[\frac{3r(h-y)}{R^5s} + \frac{3r(h-y)}{cR^4} + \frac{r(h-y)s}{c^2R^3} \right] \quad (4.1)$$

$$dE_y(r, y, s) = \frac{dy}{4\pi\epsilon_0} I(y, s) \times \exp\left(-\frac{Rs}{s}\right) \left[\frac{2(h-y)^2 - r^2}{R^5s} + \frac{2(h-y)^2 - r^2}{cR^4} + \frac{r^2s}{c^2R^3} \right] \quad (4.2)$$

$$dB(r, y, s) = \frac{\mu_0 dy}{4\pi} I(y, s) \exp\left(-\frac{Rs}{s}\right) \left[\frac{r}{R^3} + \frac{r}{cR^2} \right] \quad (4.3)$$

where $I(y, s)$ is the Laplace domain image of the lightning channel current, h is the height of the line, c is the speed of light in free space, and r is the horizontal distance

between a point of the line along the lightning channel and the z axis. The current from the lightning channel propagating towards the cloud is defined from the modified transmission line model with exponential decay (MTLE) as follows [35]:

$$I(y, s) = \exp(-\alpha y) \exp\left(-\frac{ys}{v}\right) I(0, s) \quad (4.4)$$

where $I(0, s)$ is the initial current (channel current at ground level), v and α are the velocity and the attenuation constant of the current in vertical direction (towards the cloud), respectively. By numerical integration of (4.2), (4.3), and (4.3) from H to $-H$, where H is the height of the cloud (see Figure 4.1), the field components corresponding to the complete lightning channel are obtained. In order to consider the ground of finite conductivity, Cooray-Rubinstein expression is applied [36]

$$\tilde{E}_r(r, y, s) = E_r(r, y, s) - \frac{cB(r, 0, s)}{\sqrt{\epsilon_{rg} + 1/(\epsilon_0 \rho_g s)}} \quad (4.5)$$

where $\tilde{E}_r(r, y, s)$ is the horizontal electric field, $B(r, 0, s)$ is the magnetic field at ground level assuming ground is a perfect conductor, ρ_g is the ground resistivity, and ϵ_{rg} is the relative ground permittivity.

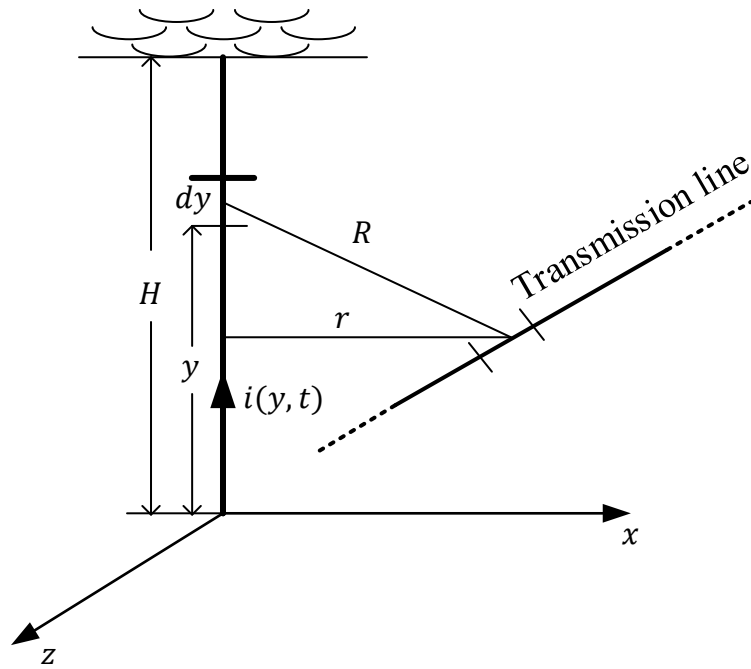


Figure 4.1 Geometrical configuration for the electromagnetic coupling between the lightning channel and a transmission line

4.3 Description of General Code

The general code is divided in single phase line and multiconductor line. The block diagram from Fig. 4.2 shows the steps for using the code. Each step is explained in detail below.

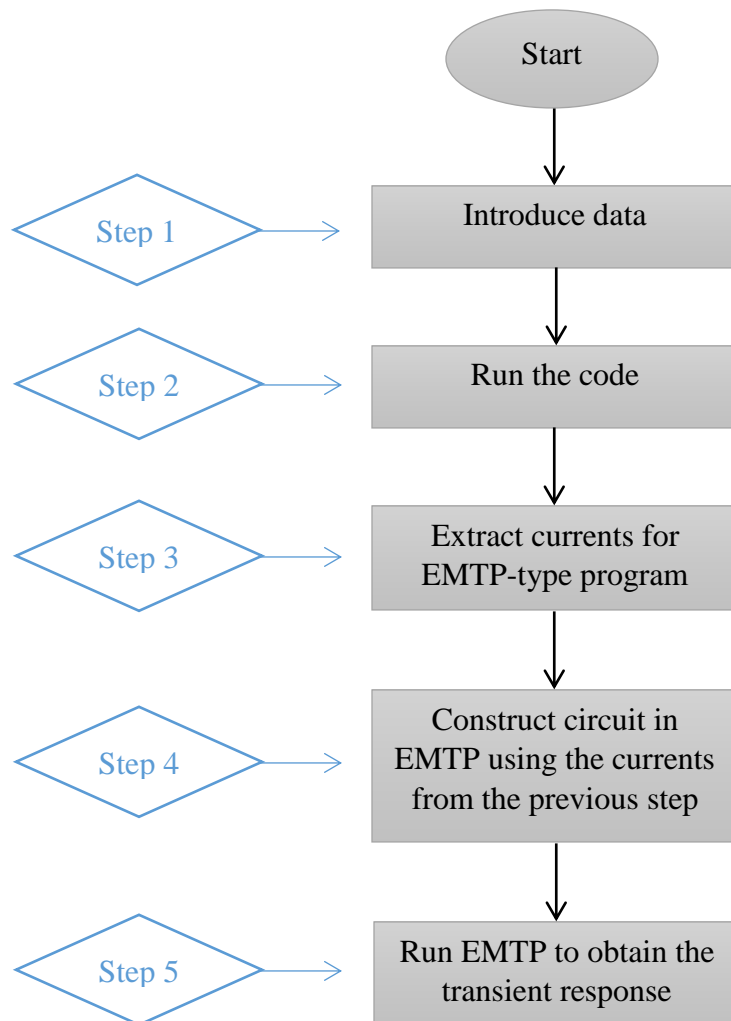


Figure 4.2 Block diagram for the general code

Step 1 Introduce data.

The data introduced in this step are listed below:

- 1- Parameters related to the transmission line: Height of the line, length of the line, conductor radius, distance between phases (for multiconductor line), ground resistivity, and conductor resistivity.
- 2- Data related to simulation process: Number of discrete samples (N) and simulation time (T).
- 3- Data related to lightning channel: Cloud's height, and coordinates of the point of stroke impact $P(z_p, x_p)$, which are measured from the sending node of the line, as shown in Figure 4.3 [26].

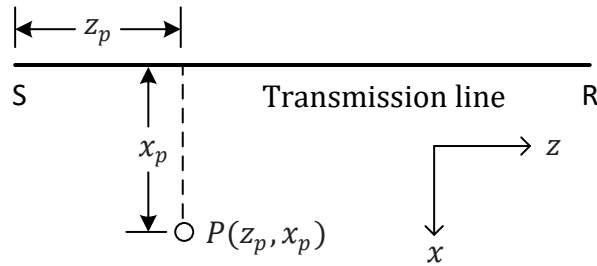


Figure 4.3 Coordinates of the point of impact

Step 2 Run the code.

After running the code, current sources will be saved automatically in the format required by the simulation program. No further input is required from the user at this step.

Step 3 Extract currents for EMTP-type program.

For the single phase line code, there are two text files corresponding to current source vectors that are saved in the main folder (the folder where the Matlab file is saved). These files are used in ATP or PSCAD as terminal current sources connected at the ends of the line.

For the multiconductor line case, six text files corresponding to current source vectors are generated. Three of them are for the sending node (one for each phase), and the three remaining files are for the receiving node. The inclusion of these text files in ATP or PSCAD for single phase and multiconductor lines is explained in the next step.

Step 4 Construct circuit in EMTP using the currents from the previous step.

For ATP, the procedure is as follows:

- 1- Select the line model (LCC) and enter the same line parameters from Step 1.
- 2- At the ends of the line, add matching resistors with the value computed according to (4.6). These resistors should be grounded, as shown in Figures 4.4 and 4.5.

$$Z_S = Z_L = 60 \log\left(\frac{2h}{r}\right) \quad (4.6)$$

In (4.6) Z_S and Z_L represent source and load resistors connected at the ends of the line to avoid reflections, h is the height of conductor, and r is the conductor radius.

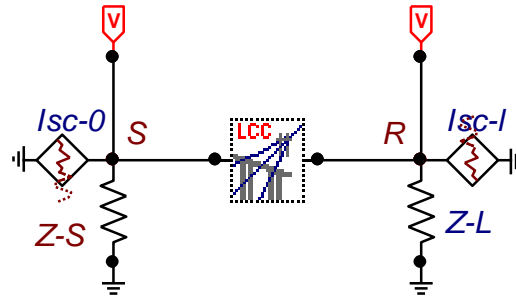


Figure 4.4 Circuit developed in ATP for an illuminated single phase line

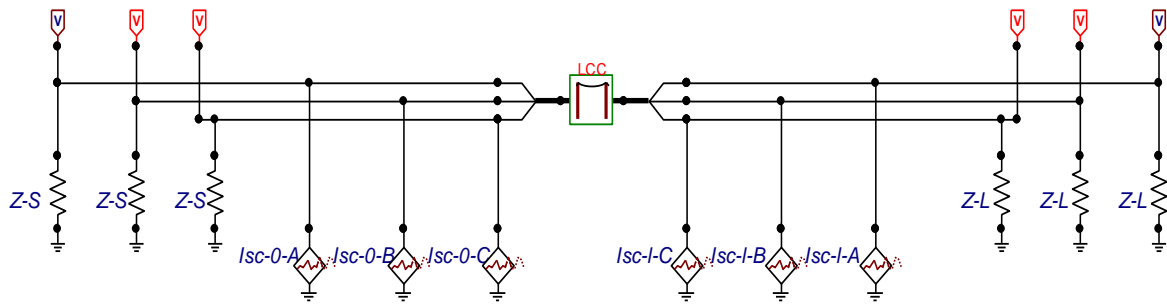


Figure 4.5 Circuit developed in ATP for an illuminated multiconductor line

- 3- Add “empirical type 1” sources at the ends of the line as shown in Figures 4.4 and 4.5. Then, use the text files from Step 3 as input data for the sources, as explained below:
 - a- Go to the characteristic section from each “empirical type 1” source (Figure 4.6).

- b- Check the “include characteristic” box. Then, from the “external characteristic” section (bottom), click on “edit”, as shown in Figure 4.6.

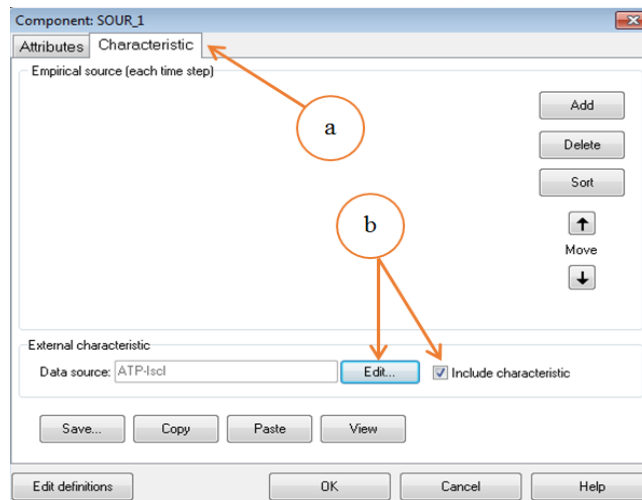


Figure 4.6 Steps a and b for the inclusion of external currents from text file in ATP

- c- A new window will open, as shown in Figure 4.7. Click on “import” from the “file” drop-down menu. Open the text file described in Step 3, then click on “done”.

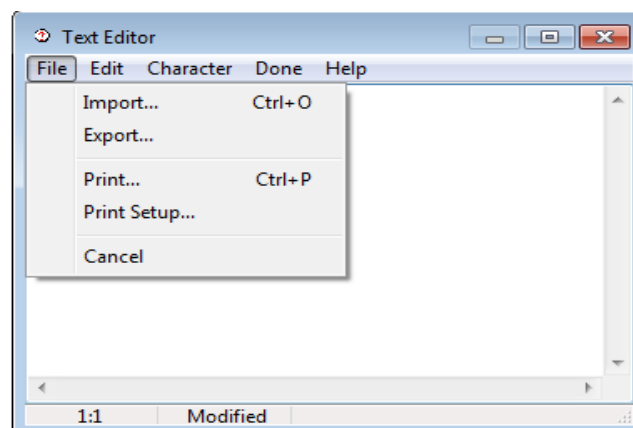


Figure 4.7 Step c for the inclusion of external currents from text file in ATP

For PSCAD, the procedure is as follows:

- 1- Select the line model (TLine_1) and enter the same line parameters from Step 1.
- 2- At the ends of the line, add matching resistors, similarly to the procedure used for ATP (see Figures 4.8 and 4.9).

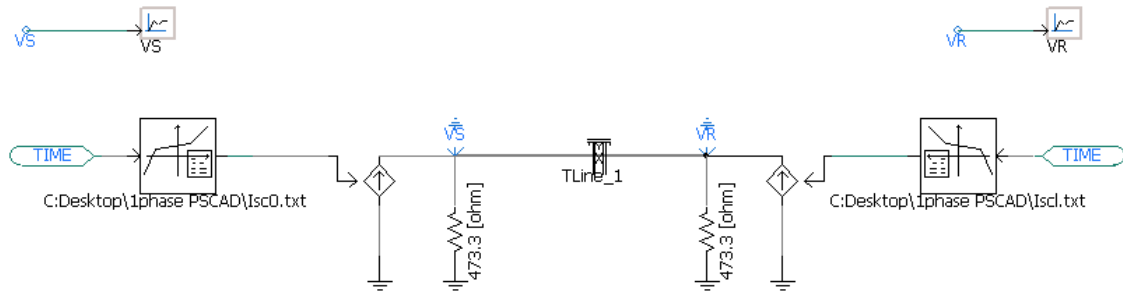


Figure 4.8 Circuit developed in PSCAD for an illuminated single phase line

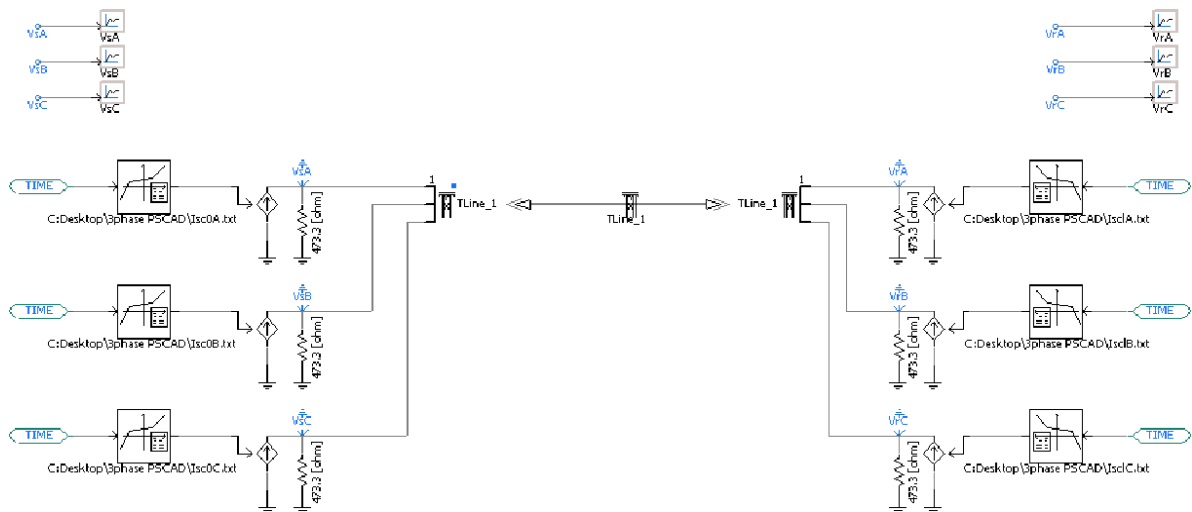


Figure 4.9 Circuit developed in PSCAD for an illuminated multiconductor line

- 3- Add current sources at the ends of the line as shown in Figures 4.8 and 4.9. Then, connect an “X-Y Transfer Function” to each source to include the text files saved in step 3, as explained below:
- a- Open the current source and select “Yes” for “External Control”, as shown in Figure 4.10.

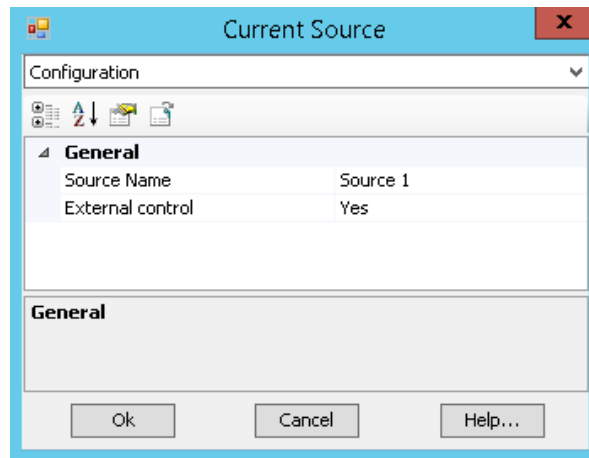


Figure 4.10 Step a for the inclusion of external currents from text file in PSCAD

- b- Open the X-Y Transfer Function and choose “File” from “Data entry method”, as shown in Figure 4.11.
- c- From the drop-down menu in the X-Y Transfer Function select “Data - filename”.

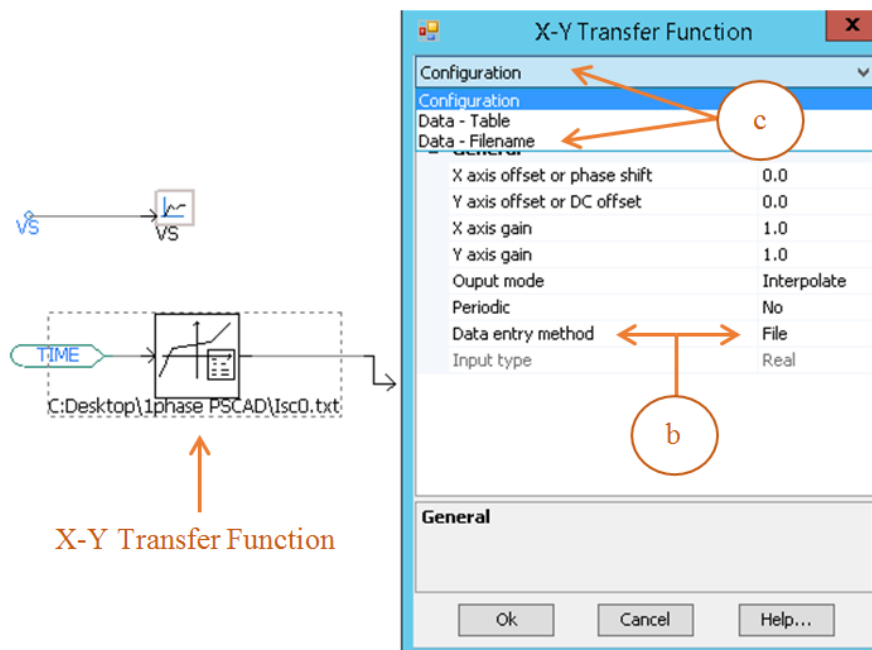


Figure 4.11 Steps b and c for the inclusion of external currents from text file in PSCAD

- d- From “Data - filename”, use “Absolute Pathname” to provide each text file name as an absolute path (e.g. C:\filename.txt), as illustrated in Figure 4.12.

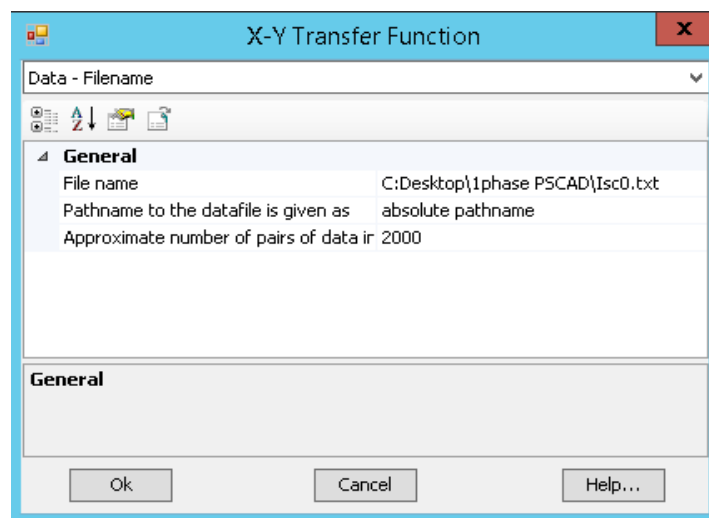


Figure 4.12 Step d for the inclusion of external currents from text file in PSCAD

For the multiconductor case, resistors and terminal current sources should be included per conductor at both ends of the line, as shown in Figures 4.5 and 4.9.

Step 5 Run EMTP-type program to obtain the transient response

After performing Steps 1 to 4, the EMTP-type program is ready to run in order to obtain the transient response. The user should use the same time step and simulation time used in the general code.

4.4 Test Case in ATP Program and Validation with NLT

The general code is used in the following application examples to simulate the effect of indirect lightning on transmission lines. Single phase and multiconductor line cases are considered, comparing the results from each EMTP-type program (ATP and PSCAD) with those from the frequency domain method and the application of the numerical Laplace transform (NLT).

4.4.1 Application Example for Single Phase Line in ATP

This application example corresponds to a single phase line with the parameters listed in Table 4.1. The line is excited by an indirect lightning stroke according to the parameters from Table 4.2. An observation time of 9.5 μ s and a number of samples of 1024 are considered for the simulations. Using the configuration shown in Figure 4.3, three different points of impact for the lightning stroke are simulated, as shown in Table 4.2. Figures 4.13, 4.14, and 4.15 show the transient voltage obtained at the sending and

receiving nodes of the line (S and R, respectively); the results from NLT and ATP are very similar.

Table 4.1 Parameters for single phase line

Line length	500 m
Line height	10 m
Conductor radius	0.0075 m
Ground resistivity	100 $\Omega\cdot\text{m}$
Conductor resistivity	3.21×10^{-8} $\Omega\cdot\text{m}$

Table 4.2 Lightning channel data

Height of cloud	1200 m
Coordinate from point of impact z_p	150, 300, 400 m
Coordinate from point of impact x_p	50, 60, 70 m

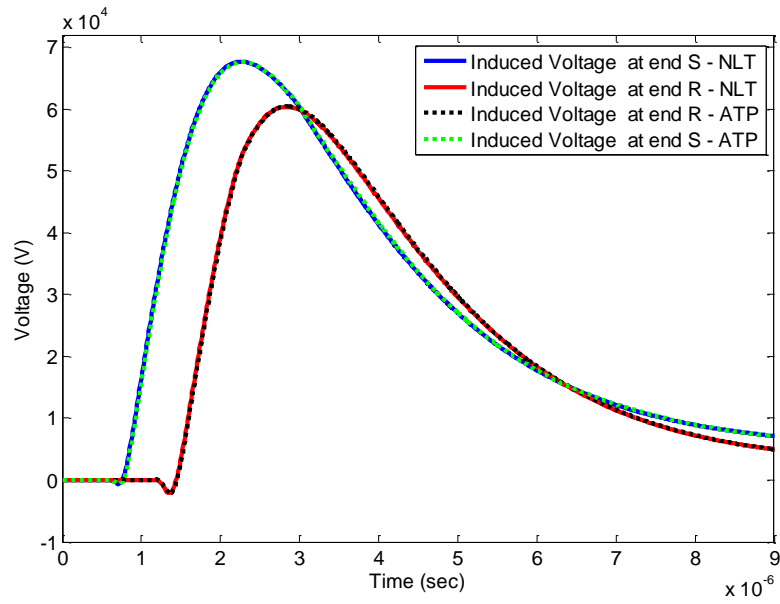


Figure 4.13 Induced voltages at the ends of a single phase line for point of impact

$P(150,50)$ - ATP

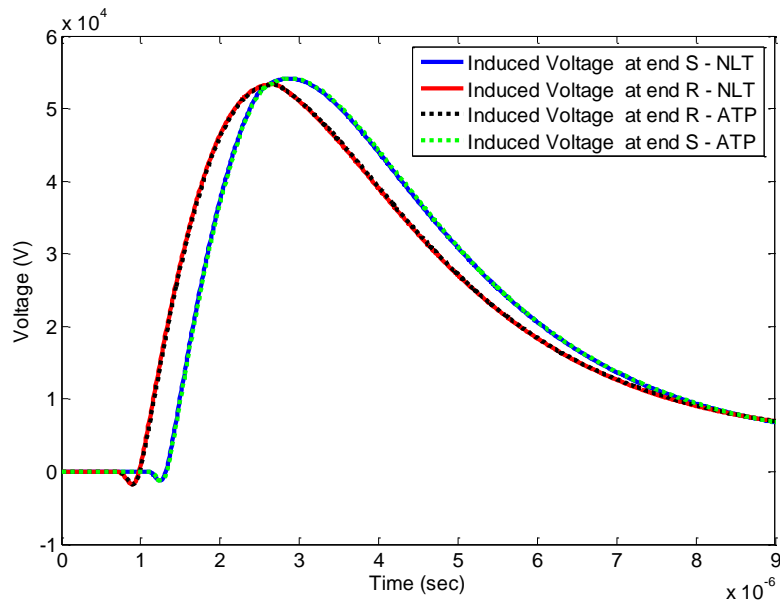


Figure 4.14 Induced voltages at the ends of a single phase line for point of impact

$P(300,60)$ - ATP

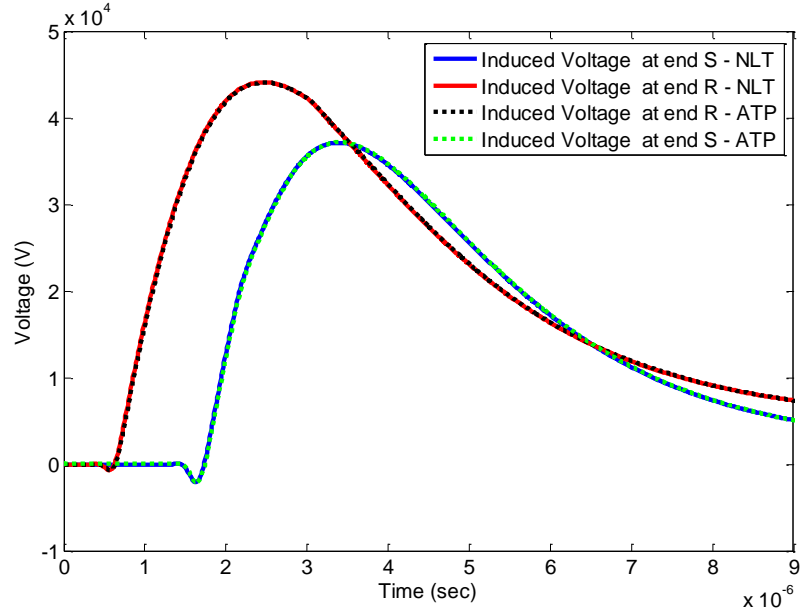


Figure 4.15 Induced voltages at the ends of a single phase line for point of impact
 $P(400,70)$ - ATP

The specific point of impact $P(z_p, x_p)$ (see Figure 4.3) affects the magnitude and waveform of the transient voltage induced in the line. As expected, the magnitude of induced voltage is larger at the node closer to the point of impact, as illustrated in Figures 4.13 to 4.15.

4.4.2 Application Example for Multiconductor Line in ATP

The general code is applied in this section to obtain the effect of indirect lightning on a multiconductor line. The main data of the line and the lightning channel for this example are listed in Tables 4.3 and 4.4, respectively. The observation time and number of samples for this test case are 10 μ s and 1024, respectively. The simulations were performed for three different values of the point of impact, as shown in Table 4.4.

According to the arrangement shown in Figure 4.3, x_p is the distance between the lightning stroke channel and the middle conductor (Phase B). Figures 4.16, 4.17 and 4.18 show the induced voltage obtained at the sending and receiving nodes. A high level of agreement between the results from ATP and NLT can be noticed.

Table 4.3 Parameters for multiconductor line

Line length	200 m
Line height	10 m
Distance between conductors	2 m
Conductor radius	0.0075 m
Ground resistivity	100 $\Omega\cdot\text{m}$
Conductor resistivity	$3.21 \times 10^{-8} \Omega\cdot\text{m}$

Table 4.4 Lightning channel data

Height of cloud	1200 m
Coordinate from point of impact z_p	25, 50, 175 m
Coordinate from point of impact x_p	50, 60, 70 m

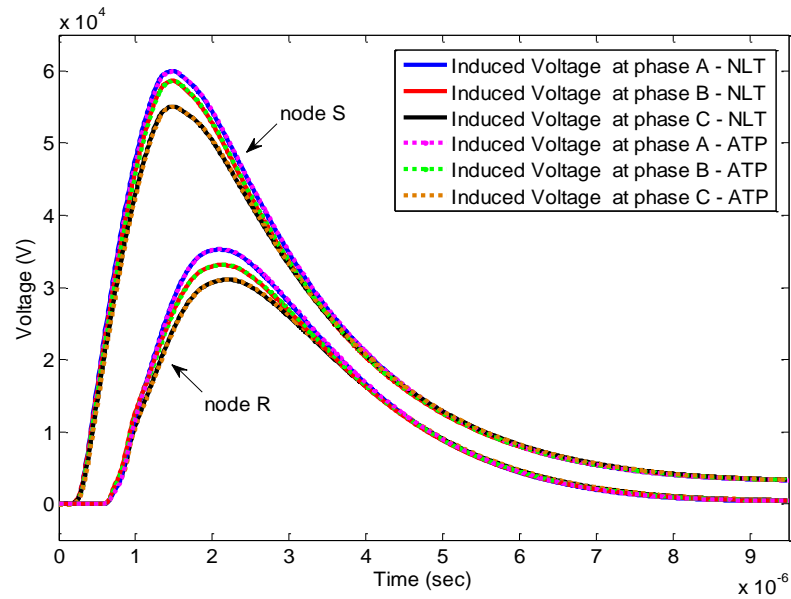


Figure 4.16 Induced voltages at the ends of a multiconductor line for point of impact

P(25,50) - ATP

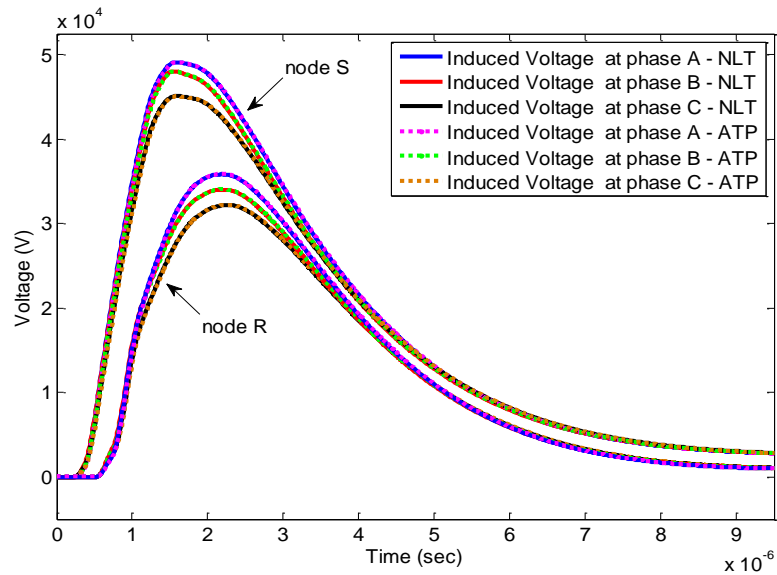


Figure 4.17 Induced voltages at the ends of a multiconductor line for point of impact

P(50,60) - ATP

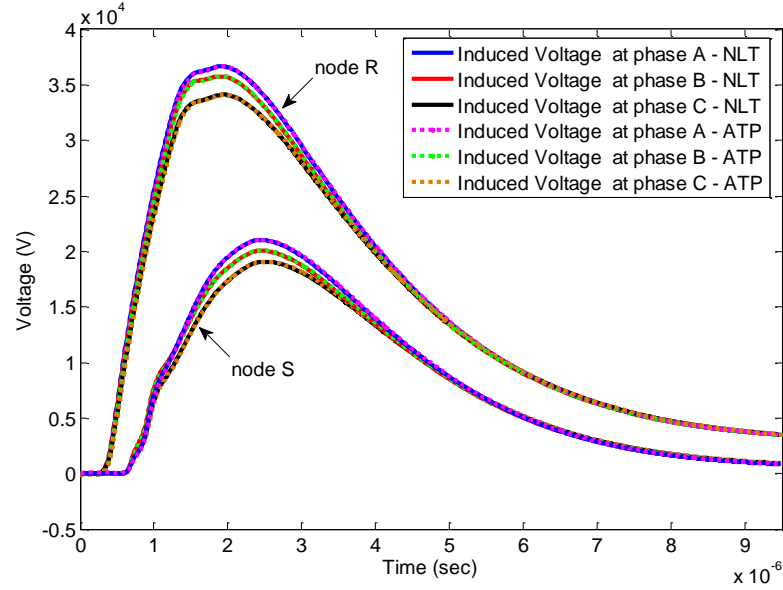


Figure 4.18 Induced voltages at the ends of a multiconductor line for point of impact

P(175,70) - ATP

4.5 Test Case in PSCAD Program and Validation with NLT

Two application examples are considered in this section. In the first application example, a single phase line is excited by indirect lightning. Then, a multiconductor line is excited by the same phenomenon. The results obtained with PSCAD are validated by means of comparisons with a frequency domain method based on the application of the NLT.

4.5.1 Application Example for Single Phase Line in PSCAD

The same line and lightning channel parameters from section 4.4.1 are considered in this section. Figures 4.19, 4.20 and 4.21 show the induced voltages obtained with PSCAD

and NLT at the ends of the line; a high level of agreement between waveforms can be observed.

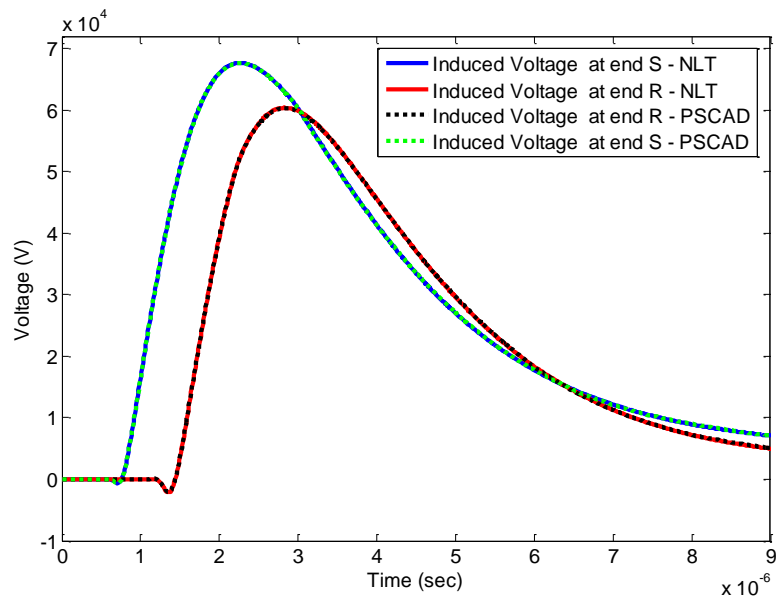


Figure 4.19 Induced voltages at the ends of a single phase line for point of impact
P(150,50) - PSCAD

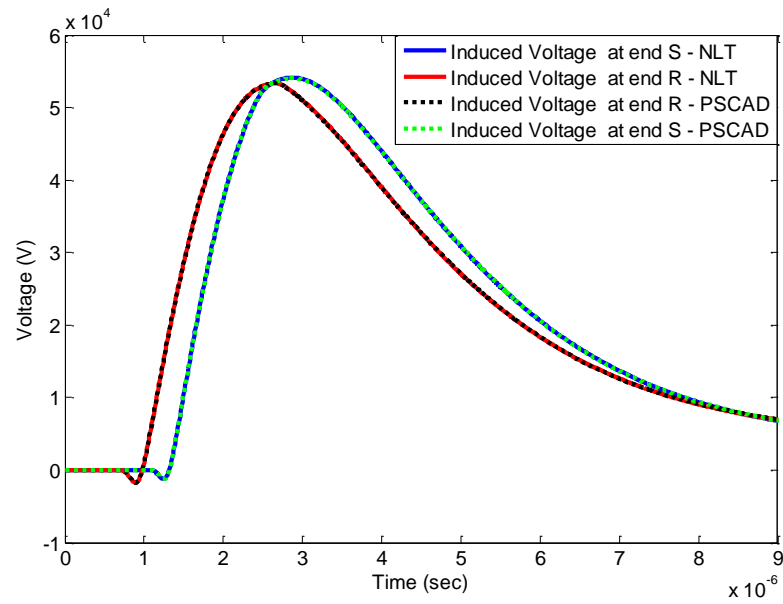


Figure 4.20 Induced voltages at the ends of a single phase line for point of impact

P(300,60) - PSCAD

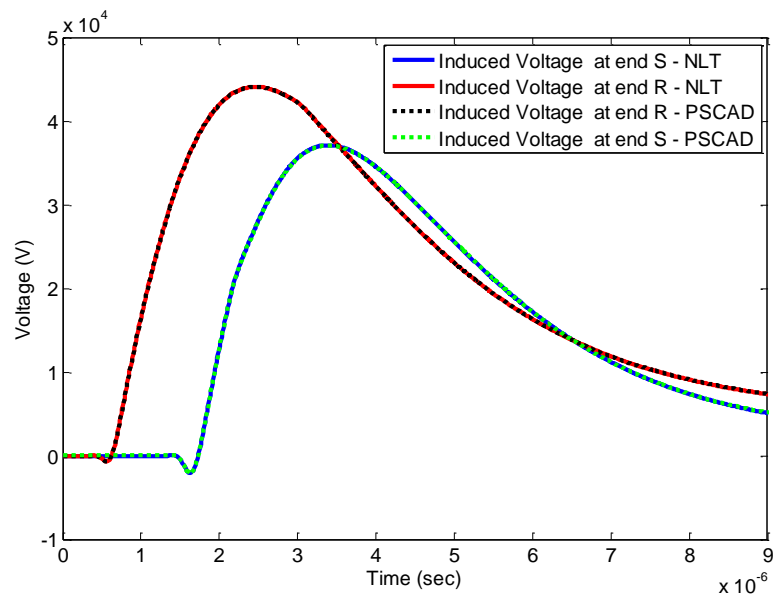


Figure 4.21 Induced voltages at the ends of a single phase line for point of impact

P(400,70) - PSCAD

4.5.2 Application Example for Multiconductor Line in PSCAD

In this application example, the same parameters for the line and lightning channel used in section 4.4.2 are considered. Figures 4.22, 4.23 and 4.24 show the induced voltages obtained with PSCAD and NLT at the sending and receiving nodes. Similarly to the previous examples, the results from both simulation methods are very similar.

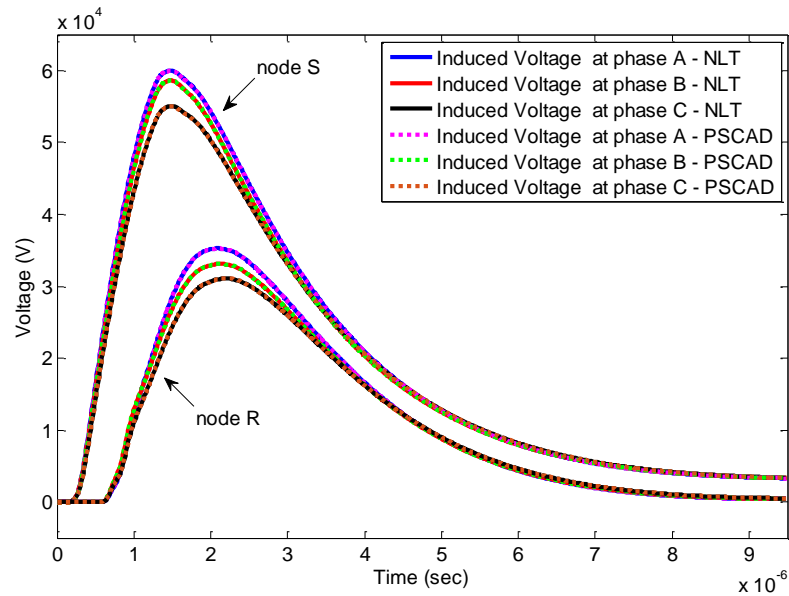


Figure 4.22 Induced voltages at the ends of a multiconductor line for point of impact

P(25,50) - PSCAD

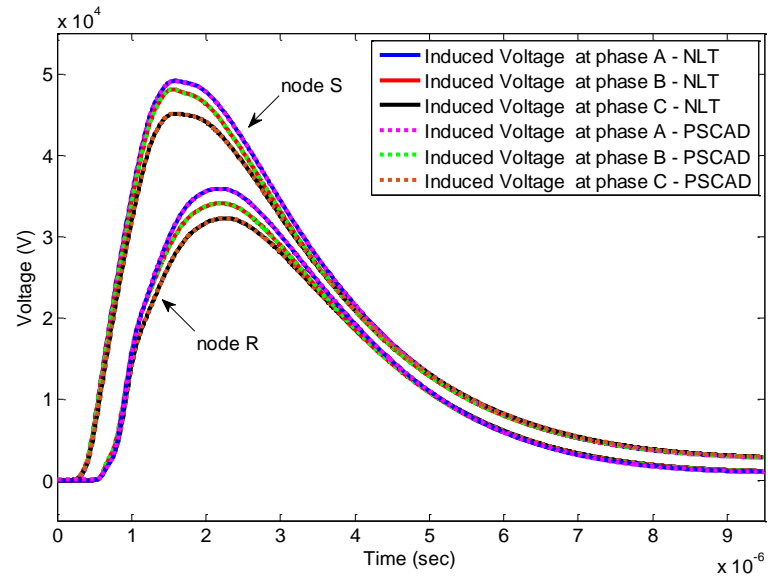


Figure 4.23 Induced voltages at the ends of a multiconductor line for point of impact

$P(50,60)$ - PSCAD

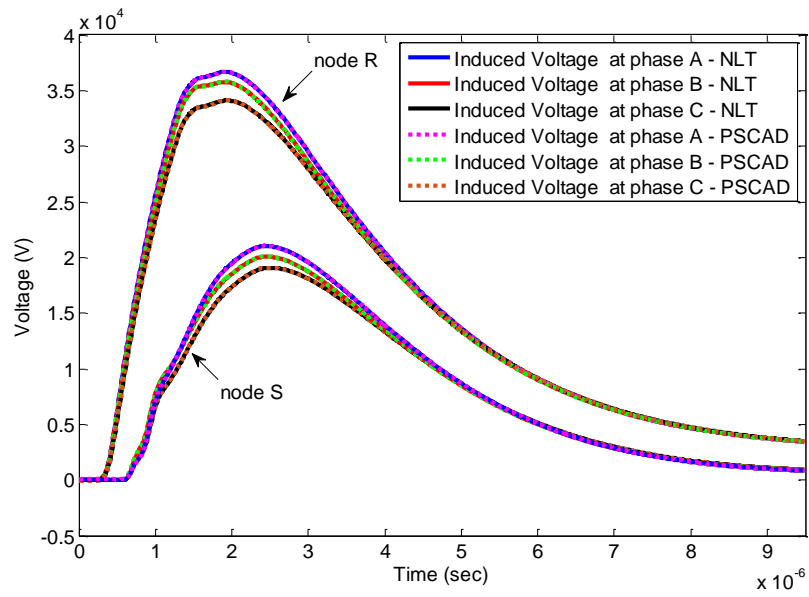


Figure 4.24 Induced voltages at the ends of a multiconductor line for point of impact

$P(175,70)$ - PSCAD

4.6 Conclusions

This chapter described the computation of incident electromagnetic fields from indirect lightning. A description of the general code implemented for this purpose was presented step by step. In order to obtain the effect of electromagnetic coupling between a transmission line and an indirect lightning stroke, several application examples were performed using transient simulation programs ATP and PSCAD, comparing the results with a frequency domain method based on the numerical Laplace transform. According to the results from all cases, a high level of agreement between the results from the EMTP-type programs and the frequency domain model were observed.

CHAPTER 5

CONCLUSIONS AND FUTURE WORK

The simulation of the effect of indirect lightning on transmission lines is very important for the design of insulation and protection elements. This thesis presents and implements a general code to calculate the effect of nearby lightning strokes on transmission lines. The explanation of the general code follows the block diagram presented in Chapter 4. The main objective of the general code is to obtain terminal currents sources representing electromagnetic fields induced by indirect lightning and use them as external sources for the simulation programs ATP and PSCAD. The illuminated transmission line model described in Chapter 3 is applied to create the general code. The results from this thesis yield the following conclusions:

- 1- According to the comparisons provided, the results from the general code match those from the frequency domain method used as base solution for all the cases considered.
- 2- The user of the general code does not require a deep knowledge of the model definition, parameter computation or numerical tools used. It is sufficient to introduce the correct inputs, run the code and apply the resulting files as external current sources in the software selected (PSCAD or ATP), as explained in Chapter 4 of this thesis.

- 3- The general code allows considering the effect of an indirect lightning stroke impacting the ground at any point near the line, and for different types of transmission line configurations.
- 4- According to the results from Chapter 4, the point of impact $P(z_p, x_p)$ of the lightning stroke affects the magnitude and waveform of the induced transient voltage. The voltage magnitude is larger at the node closer to the point of impact for the cases under consideration.

The following points are some recommendations for future work:

- 1- Include surge arresters in the simulations.
- 2- Include ground wires in the tower configurations.
- 3- Extend the general code to nonuniform transmission lines (sagging between towers).
- 4- Besides the horizontal tower configuration (all phases placed at the same height above ground), extend the proposed method to other configurations.

BIBLIOGRAPHY

- [1] P. Chowdhuri, *Electromagnetic Transients in Power Systems*, New Delhi: Asoke K. Ghosh, 2004.
- [2] M. J. Master and M. A. Uman, "Lightning Induced Voltages on Power Lines: Theory," *IEEE Transactions on Power Apparatus and Systems*, vol. PAS-103, no. 9, pp. 2502 - 2518, 1984.
- [3] P. Gómez and J. C. Escamilla, "Frequency domain modeling of nonuniform multiconductor lines excited by indirect lightning," *International Journal of Electrical Power & Energy Systems*, vol. 45, no. 1, p. 420–426, 2013.
- [4] P. Gómez, "Non Uniform Transmission Line Modeling for Electromagnetic Transient Analysis," CINVESTAV del I.P.N., Guadalajara, 2005.
- [5] C. Taylor and C. J. Harrison, "The response of a terminated two-wire transmission line excited by a nonuniform electromagnetic field," *IEEE Transactions on Antennas and Propagation*, vol. 13, no. 6, pp. 987 - 989, 1965.
- [6] C. R. Paul, "Frequency Response of Multiconductor Transmission Lines Illuminated by an Electromagnetic Field," *IEEE Transactions on Electromagnetic Compatibility*, vol. EMC-18, no. 4, pp. 183 - 190, 1976.
- [7] A. K. Agrawal, H. J. Price and S. H. Gurbaxani, "Transient Response of Multiconductor Transmission Lines Excited by a Nonuniform Electromagnetic Field," *IEEE Transactions on Electromagnetic Compatibility*, vol. EMC-22, no. 2, pp. 119 - 129, 1980.
- [8] F. Rachidi, "Formulation of the field-to-transmission line coupling equations in terms of magnetic excitation field," *IEEE Transactions on Electromagnetic Compatibility*, vol. 35, no. 3, pp. 404 - 407, 1993.
- [9] V. Cooray, "Calculating lightning-induced overvoltages in power lines. A comparison of two coupling models," *IEEE Transactions on Electromagnetic Compatibility*, vol. 36, no. 3, pp. 179 - 182, 1994.
- [10] S. Rusck, "Induced lightning over-voltages on power-transmission lines with special reference to the over-voltage protection of low-voltage networks," *Transactions of the Royal Institute of Technology*, Stockholm, no. 120, 1958.

- [11] C. R. Paul, "A SPICE model for multiconductor transmission lines excited by an incident electromagnetic field," *IEEE Transactions on Electromagnetic Compatibility*, vol. 36, no. 4, pp. 342 - 354, 1994.
- [12] C. R. Paul, "Literal solutions for the time-domain response of a two-conductor transmission line excited by an incident electromagnetic field," *IEEE Transactions on Electromagnetic Compatibility*, vol. 37, no. 2, pp. 241 - 251, 1995.
- [13] C. A. Nucci, F. Rachidi, M. Ianoz and C. Mazzetti, "Comparison of two coupling models for lightning-induced overvoltage calculations," *IEEE Transactions on Power Delivery*, vol. 10, no. 1, pp. 330 - 339, 1995.
- [14] M. Omid, Y. Kami and M. Hayakawa, "Field coupling to nonuniform and uniform transmission lines," *IEEE Transactions on Electromagnetic Compatibility*, vol. 39, no. 3, pp. 201 - 211, 1997.
- [15] V. Cooray and V. Scuka, "Lightning-induced overvoltages in power lines: validity of various approximations made in overvoltage calculations," *IEEE Transactions on Electromagnetic Compatibility*, vol. 40, no. 4, pp. 355 - 363, 1998.
- [16] I. Erdin , A. Dounavis, R. Achar and M. S. Nakhla, "A SPICE model for incident field coupling to lossy multiconductor transmission lines," *IEEE Transactions on Electromagnetic Compatibility* , vol. 43, no. 4, pp. 485 - 494, 2001.
- [17] P. Gomez, P. Moreno and J. L. Naredo, "Frequency-domain transient analysis of nonuniform lines with incident field excitation," *IEEE Transactions on Power Delivery*, vol. 20, no. 3, pp. 2273 - 2280, 2005.
- [18] G. Shinh , N. Nakhla, R. Achar, M. Nakhla and I. Erdin, "Analysis of multiconductor transmission lines with frequency-dependent parameters and incident electromagnetic fields," in *Microwave Symposium Digest, 2005 IEEE MTT-S International*, 2005.
- [19] G. S. Shinh , N. M. Nakhla, R. Achar, M. S. Nakhla, A. Dounavis and I. Erdin, "Fast transient analysis of incident field coupling to multiconductor transmission lines," *IEEE Transactions on Electromagnetic Compatibility*, vol. 48, no. 1, pp. 57 - 73, 2006.
- [20] R. Gouws, "Investigation and efficiency analysis of a 405 km transmission line with series compensation," in *Industrial and Commercial Use of Energy (ICUE)*, Cape Town, 2011.

- [21] C. R. Paul, *Analysis of Multiconductor Transmission Lines*, Lexington: John Wiley & Sons, 2008.
- [22] J. A. Martinez-Velasco, *Power System Transients Parameter Determination*, Boca Raton: Taylor and Francis Group, 2009.
- [23] M. S. Mamis and M. Koksai, "Lightning surge analysis using nonuniform, single-phase line model," *IEE Proceedings - Generation, Transmission and Distribution*, vol. 148, no. 1, pp. 85 - 90, 2001.
- [24] R. Nuricumbo-Guillén, P. Gómez and F. P. Espino-Cortés, "Computation of transient voltage and current profiles along illuminated multiconductor lines by means of the numerical Laplace transform," *IET Generation, Transmission & Distribution*, vol. 9, no. 13, pp. 1608 - 1613, 2015.
- [25] C. D. Taylor and J. P. Castillo, "On Electromagnetic-Field Excitation of Unshielded Multiconductor Cables," *IEEE Transactions on Electromagnetic Compatibility*, vol. EMC-20, no. 4, pp. 495 - 500, 1978.
- [26] P. Gomez and J. C. Escamilla, "Frequency domain modeling of transmission lines excited by nearby lightning strokes," in *International Conference on Power Systems Transients*, Kyoto, 2009.
- [27] J. O. S. Paulino, A. E. A. de Araujo and G. C. de Miranda, "Lightning induced voltage calculation in lossy transmission lines," *IEEE Transactions on Magnetics*, vol. 34, no. 5, pp. 2807 - 2810, 1998.
- [28] A. Ramirez, J. L. Naredo and P. Moreno, "Full frequency-dependent line model for electromagnetic transient simulation including lumped and distributed sources," *IEEE Transactions on Power Delivery*, vol. 20, no. 1, pp. 292 - 299, 2005.
- [29] A. A. Smith, "A More Convenient Form of the Equations for the Response of a Transmission Line Excited by Nonuniform Fields," *IEEE Transactions on Electromagnetic Compatibility*, vol. EMC-15, no. 3, pp. 151 - 152, 1973.
- [30] P. Moreno, P. Gomez, M. Davila and J. L. Naredo, "A Uniform Line Model for Non-Uniform Single-Phase Lines with Frequency Dependent Electrical Parameters," in *Transmission & Distribution Conference and Exposition*, Caracas, 2006.
- [31] A. J. Eriksson, D. V. Meal and . M. . F. Stringfellow, "Lightning-Induced Overvoltages on Overhead Distribution Lines," *IEEE Power Engineering Review*, vol. PER-2, no. 4, pp. 41 - 41, 1982.
- [32] V. Javor, "Electromagnetic field estimation using modified transmission line models of lightning strokes," in *Software, Telecommunications and Computer Networks*

(SoftCOM), Split, 2012.

- [33] M. Paolone, E. Perez, A. Borghetti, C. A. Nucci, F. Rachidi and H. Torres, "Comparison of Two Computational Programs for the Calculation of Lightning-Induced Voltages on Distribution Systems," in *6th International Conference on Power Systems Transients (IPST)*, Montreal, 2005.
- [34] J. A. Gutierrez Robles, "Analysis of Electromagnetic Transients due to Lightning in Transmission Towers And Distribution Lines," CINVESTAV IPN, Guadalajara, 2002.
- [35] C. A. Nucci, F. Rachidi, M. V. Ianoz and C. Mazzetti, "Lightning-induced voltages on overhead lines," *IEEE Transactions on Electromagnetic Compatibility*, vol. 35, no. 1, pp. 75 - 86, 1993.
- [36] F. Rachidi, C. A. Nucci, . M. Ianoz and C. Mazzetti, "Influence of a lossy ground on lightning-induced voltages on overhead lines," *IEEE Transactions on Electromagnetic Compatibility* , vol. 38, no. 3, pp. 250 - 264, 1996.
- [37] P. Moreno and A. Ramirez, "Implementation of the Numerical Laplace Transform: A Review," *IEEE Transactions on Power Delivery*, vol. 23, no. 4, pp. 2599 - 2609, 2008.
- [38] R. Nuricumbo-Guillén, P. Gómez, F. P. Espino-Cortés and F. A. Uribe, "Accurate Computation of Transient Profiles Along Multiconductor Transmission Systems by Means of the Numerical Laplace Transform," *IEEE Transactions on Power Delivery*, vol. 29, no. 5, pp. 2385 - 2393, 2014.
- [39] P. Gómez and F. A. Uribe, "The numerical Laplace transform: An accurate technique for analyzing electromagnetic transients on power system devices," *International Journal of Electrical Power & Energy Systems*, vol. 31, no. 2-3, p. 116–123, 2009.
- [40] P. Moreno, P. Gómez, J. L. Naredo and J. L. Guardado, "Frequency domain transient analysis of electrical networks including non-linear conditions," *International Journal of Electrical Power & Energy Systems*, vol. 27, no. 2, p. 139–146, 2005.
- [41] C. R. Paul, "Decoupling the multiconductor transmission line equations," *IEEE Transactions on Microwave Theory and Tech.*, vol. 44, no. 8, pp. 1429 - 1440.

Appendix A: Electrical Parameters of the Transmission Line

A.1 Introduction

An adequate parameter computation is an essential component of transmission line modeling and simulation. For multiconductor lines, these parameters correspond to impedance and admittance matrices [4].

A.2 Impedance Matrix

The impedance matrix can be divided in three terms:

$$\mathbf{Z} = \mathbf{Z}_g + \mathbf{Z}_e + \mathbf{Z}_c \quad (\text{A.1})$$

where \mathbf{Z}_g is the geometric impedance matrix, \mathbf{Z}_e is the earth return impedance matrix, and \mathbf{Z}_c is the conductor impedance matrix.

A.2.1 Geometric Impedance

The geometric impedance is given by:

$$\mathbf{Z}_g = j\omega \frac{\mu_o}{2\pi} \mathbf{P} \quad (\text{A.2})$$

where ω is the angular frequency, μ_o is the free space permeability, and \mathbf{P} is a matrix of geometrical coefficients, defined as:

$$\mathbf{P} = \begin{bmatrix} \ln \frac{D_{11}}{R_{eq,i}} & \dots & \ln \frac{D_{1n}}{d_{1n}} \\ \vdots & \ddots & \vdots \\ \ln \frac{D_{n1}}{d_{n1}} & \dots & \ln \frac{D_{nn}}{R_{eq,i}} \end{bmatrix} \quad (\text{A.3})$$

Applying the method of images, as shown in figure A.1, the variables in (A.3) are defined as follows:

$$D_{ij} = \sqrt{(x_i - x_j)^2 + (y_i + y_j)^2} \quad (\text{A.4})$$

$$d_{ij} = \sqrt{(x_i - x_j)^2 + (y_i - y_j)^2} \quad (\text{A.5})$$

$$R_{eq,i} = \sqrt[n]{n r_i (r_h)^{n-1}} \quad (\text{A.6})$$

where x_i and y_i are the coordinates of the i th phase conductor, n is the number of conductors in a bundle, $R_{eq,i}$ is the equivalent radius of the i th phase bundle, r_i, r_h are the radius of the i th phase conductor and the bundle radius, respectively.

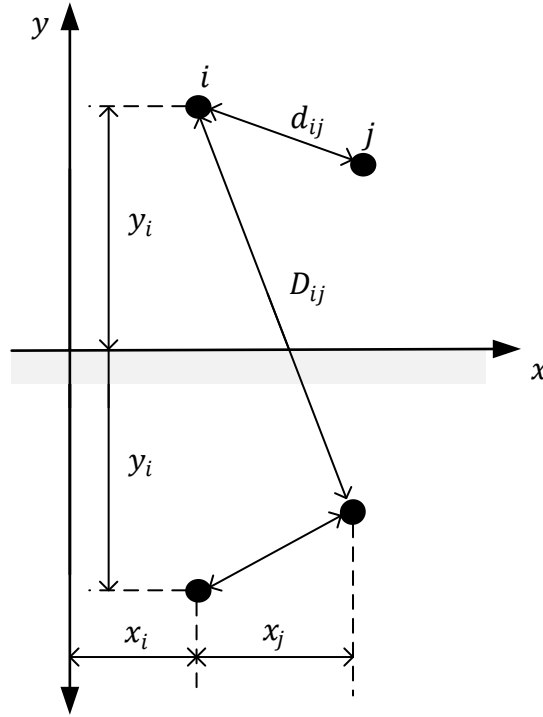


Figure A.1 Method of images

A.2.2 Earth Return Impedance

To compute the earth return impedance, the method of the complex penetration depth is applied, as shown in figure A.2. This yields:

$$\mathbf{Z}_e = j\omega \frac{\mu_o}{2\pi} \begin{bmatrix} \ln \frac{D'_{11}}{D_{11}} & \dots & \ln \frac{D'_{1n}}{D_{1n}} \\ \vdots & \ddots & \vdots \\ \ln \frac{D'_{n1}}{D_{n1}} & \dots & \ln \frac{D'_{nn}}{D_{nn}} \end{bmatrix} \quad (\text{A.7})$$

where

$$D'_{ij} = \sqrt{(x_i - x_j)^2 + (y_i + y_j + 2p)^2} \quad (\text{A.8})$$

Complex penetration depth p is given by:

$$p = \sqrt{\frac{\rho_e}{j\omega\mu_e}} \quad (\text{A.9})$$

where ρ_e is the ground resistivity and μ_e is the ground permeability.

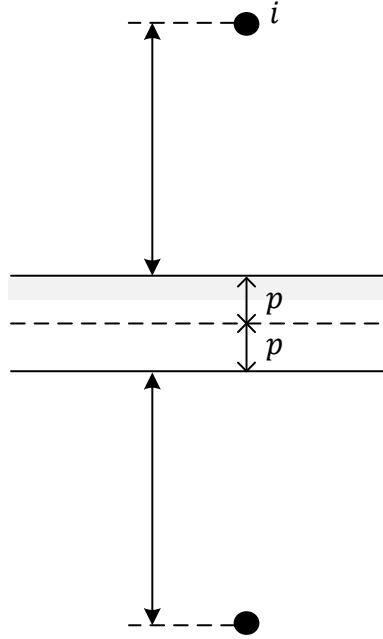


Figure A.2 Penetration depth representation

A.2.3 Conductor Impedance

The internal conductor impedance is due to the dc resistive component and the skin effect phenomenon. The complex penetration depth in the conductor is defined as follows:

$$p_c = \sqrt{\frac{\rho_c}{j\omega\mu_c}} \quad (\text{A.10})$$

The impedance of the i th phase conductor is defined by:

$$Z_{c,i} \cong \frac{\sqrt{R_{dc,i}^2 + Z_{hf,i}^2}}{n} \quad (\text{A.11})$$

where $R_{dc,i}$ and $Z_{hf,i}$ are the direct current resistance and high frequency impedance of the i th phase conductor, respectively. These terms are defined as follows:

$$R_{dc,i} = \frac{\rho_{c,i}}{\pi r_i^2} \quad (\text{A.12})$$

$$Z_{hf,i} = \frac{\rho_{c,i}}{2\pi r_i p_c} \quad (\text{A.13})$$

where $\mu_{c,i}$ and $\rho_{c,i}$ are the permeability and resistivity of the i th phase conductor, respectively. The conductor impedance matrix of the line is defined by:

$$\mathbf{Z}_c = \text{diag} (Z_{c,1}, Z_{c,2}, \dots, Z_{c,n}) \quad (\text{A.14})$$

A.3 Admittance Matrix

The admittance matrix is computed from \mathbf{P} and the permittivity of free space ϵ_0 as follows:

$$\mathbf{Y} = j\omega 2\pi\epsilon_0 \mathbf{P}^{-1} \quad (\text{A.15})$$

Appendix B: Numerical Laplace Transform

The numerical Laplace transform (NLT) is applied to obtain the time domain response of the frequency domain models described in this thesis [37]-[40].

The time domain signal $f(t)$ and the frequency domain signal $F(s)$ are related by the Laplace transform as follows:

$$F(s) = \int_0^{\infty} f(t)e^{-st} dt \quad (\text{B.1})$$

while the inverse Laplace transform is:

$$f(t) = \frac{1}{2\pi j} \int_{c-j\infty}^{c+j\infty} F(s)e^{st} ds \quad (\text{B.2})$$

where s is the complex frequency given by:

$$s = c + j\omega \quad (\text{B.3})$$

being c is a positive real constant, and ω is the angular frequency. Equations (B.1) and (B.2) can be expressed as:

$$F(s) = \int_0^{\infty} [f(t)e^{-ct}]e^{-j\omega t} dt \quad (\text{B.4})$$

and

$$f(t) = \frac{e^{ct}}{2\pi} \int_{-\infty}^{+\infty} F(s) e^{j\omega t} d\omega \quad (\text{B.5})$$

When considering the numerical inversion of the Laplace transform, Gibbs oscillations are introduced due to the truncation of the integration range. The Hanning window (σ) is used to reduce these errors, according to the following expression:

$$\sigma = 0.5 \left[1 + \cos \left(0.5\pi \frac{1+n}{N} \right) \right] \quad (\text{B.6})$$

In addition, the discretization of the frequency spectrum introduces another type of error, known as aliasing error. This is reduced by defining the correct damping factor c [41]. The following value of c is used in this thesis:

$$c = 2\Delta w \quad (\text{B.7})$$

The discretization is performed considering an odd sampling with spacing $2\Delta w$ for the frequency domain samples, and regular time steps of Δt for the time domain samples. The corresponding discrete functions in time and frequency domain are:

$$f_n \equiv f(n\Delta t), \quad \text{for } n = 0, 1, \dots, N-1 \quad (\text{B.8})$$

and

$$F_{2k+1} \equiv F(c + j(2k+1)\Delta w), \quad \text{for } k = 0, 1, \dots, N-1 \quad (\text{B.9})$$

where N is the number of equally spaced samples. The minimum useful time step can be defined by:

$$\Delta t = T/N \quad (\text{B.10})$$

being T the observation time. Including the window function, the inverse numerical Laplace transform can be defined as:

$$f_n = \frac{e^{cn\Delta t}}{\pi} \operatorname{Re} \left\{ 2 \sum_{k=0}^{N-1} F_{2k+1} \sigma_{2k+1} e^{j(2k+1)n\Delta w\Delta t} \Delta w \right\} \quad (\text{B.11})$$

Substitution of (B.8) and (B.10) into (B.12) yields

$$f_n = \operatorname{Re} \left\{ C_n \left[\sum_{k=0}^{N-1} F_{2k+1} \sigma_{2k+1} e^{j2\pi kn/N} \right] \right\} \quad (\text{B.12})$$

where

$$C_n = 2N e^{cn\Delta t} e^{j\pi n/N} \Delta w / \pi \quad (\text{B.13})$$

The numerical form inside the square brackets of equation (B.12) allows the use of the Fast Fourier Transform (FFT) algorithm [37].